Published for SISSA by Springer

Received: October 5, 2012
Revised: November 9, 2012
Accepted: December 2, 2012
Published: January 3, 2013

ATLAS search for new phenomena in dijet mass and angular distributions using pp collisions at $\sqrt{s} = 7$ TeV

The ATLAS collaboration

E-mail: atlas.publications@cern.ch

Abstract: Mass and angular distributions of dijets produced in LHC proton-proton collisions at a centre-of-mass energy $\sqrt{s} = 7$ TeV have been studied with the ATLAS detector using the full 2011 data set with an integrated luminosity of $4.8\,\text{fb}^{-1}$. Dijet masses up to ~ 4.0 TeV have been probed. No resonance-like features have been observed in the dijet mass spectrum, and all angular distributions are consistent with the predictions of QCD. Exclusion limits on six hypotheses of new phenomena have been set at 95% CL in terms of mass or energy scale, as appropriate. These hypotheses include excited quarks below 2.83 TeV, colour octet scalars below 1.86 TeV, heavy W bosons below 1.68 TeV, string resonances below 3.61 TeV, quantum black holes with six extra space-time dimensions for quantum gravity scales below 4.11 TeV, and quark contact interactions below a compositeness scale of 7.6 TeV in a destructive interference scenario.

Keywords: Hadron-Hadron Scattering

ArXiv ePrint: 1210.1718

doi:10.1007/JHEP01(2013)029

JHEP01(2013)029

Contents

JHEP01(2013)029

1 Introduction

At the CERN Large Hadron Collider (LHC), collisions with the largest momentum transfer typically result in final states with two jets of particles with high transverse momentum (p_{T}). The study of these events tests the Standard Model (SM) at the highest energies accessible at the LHC. At these energies, new particles could be produced [1, 2], new interactions between particles could manifest themselves [3–6], or interactions resulting from the unification of SM with gravity could appear in the TeV range [7–12]. These collisions also probe the structure of the fundamental constituents of matter at the smallest distance scales allowing, for example, an experimental test of the size of quarks. The models for new phenomena (NP) tested in the current studies are described in section 9.

The two jets emerging from the collision may be reconstructed to determine the two-jet (dijet) invariant mass, m_{jj}, and the scattering angular distribution with respect to the colliding beams of protons. The dominant Quantum Chromodynamics (QCD) interactions for this high-p_{T} scattering regime are t-channel processes, leading to angular distributions that peak at small scattering angles. Different classes of new phenomena are expected to modify dijet mass distribution and the dijet angular distributions as a function of m_{jj}, creating either a deviation from the QCD prediction above some threshold or an excess of events localised in mass (often referred to as a "bump" or "resonance"). Most models predict that the angular distribution of the NP signal would be more isotropic than that of QCD.

Results from previous studies of dijet mass and angular distributions [13–23] were consistent with QCD predictions. The study reported in this paper is based on pp collisions at a centre-of-mass (CM) energy of 7 TeV produced at the LHC and measured by the ATLAS detector. The analysed data set corresponds to an integrated luminosity of 4.8 fb^{-1} collected in 2011 [24, 25], a substantial increase over previously published ATLAS dijet analyses [22, 23].

A detailed description of the ATLAS detector has been published elsewhere [26]. The detector is instrumented over almost the entire solid angle around the pp collision point with layers of tracking detectors, calorimeters, and muon chambers.

High-transverse-momentum hadronic jets in the analysis are measured using a finely-segmented calorimeter system, designed to achieve a high reconstruction efficiency and an excellent energy resolution. The electromagnetic calorimetry is provided by high-granularity liquid argon (LAr) sampling calorimeters, using lead as an absorber, that are split into a barrel ($|\eta| < 1.475$)[1] and end-cap ($1.375 < |\eta| < 3.2$) regions. The hadronic calorimeter is divided into barrel, extended barrel ($|\eta| < 1.7$) and Hadronic End-Cap (HEC; $1.5 < |\eta| < 3.2$) regions. The barrel and extended barrel are instrumented with scintillator tiles and steel absorbers, while the HEC uses copper with liquid argon modules. The Forward Calorimeter region (FCal; $3.1 < |\eta| < 4.9$) is instrumented with

[1] In the right-handed ATLAS coordinate system, the pseudorapidity η is defined as $\eta \equiv -\ln \tan(\theta/2)$, where the polar angle θ is measured with respect to the LHC beamline. The azimuthal angle ϕ is measured with respect to the x-axis, which points toward the centre of the LHC ring. The z-axis is parallel to the anti-clockwise beam viewed from above. Transverse momentum and energy are defined as $p_{\mathrm{T}} = p\sin\theta$ and $E_{\mathrm{T}} = E\sin\theta$, respectively.

JHEP01(2013)029

LAr/copper and LAr/tungsten modules to provide electromagnetic and hadronic energy measurements, respectively.

2 Overview of the dijet mass and angular analyses

The dijet invariant mass, m_{jj}, is calculated from the vectorial sum of the four-momenta of the two highest p_{T} jets in the event. A search for resonances is performed on the m_{jj} spectrum, employing a data-driven background estimate that does not rely on QCD calculations.

The angular analyses employ ratio observables and normalised distributions to substantially reduce their sensitivity to systematic uncertainties, especially those associated with the jet energy scale (JES), parton distribution functions (PDFs) and the integrated luminosity. Unlike the m_{jj} analysis, the angular analyses use a background estimate based on QCD. The basic angular variables and distributions used in the previous ATLAS dijet studies [18, 22] are also employed in this analysis. A convenient variable that emphasises the central scattering region is χ. If E is the jet energy and p_z is the z-component of the jet's momentum, the rapidity of the jet is given by $y \equiv \frac{1}{2}\ln(\frac{E+p_z}{E-p_z})$. In a given event, the rapidities of the two highest p_{T} jets in the pp centre-of-mass frame are denoted by y_1 and y_2, and the rapidities of the jets in the dijet CM frame are $y^* = \frac{1}{2}(y_1 - y_2)$ and $-y^*$. The longitudinal motion of the dijet CM system in the pp frame is described by the rapidity boost, $y_B = \frac{1}{2}(y_1 + y_2)$. The variable χ is: $\chi \equiv \exp(|y_1 - y_2|) = \exp(2|y^*|)$.

The χ distributions predicted by QCD are relatively flat compared to those produced by new phenomena. In particular, many NP signals are more isotropic than QCD, causing them to peak at low values of χ. For the χ distributions in the current studies, the rapidity coverage extends to $|y^*| < 1.7$ corresponding to $\chi < 30.0$. This interval is divided into 11 bins, with boundaries at $\chi_i = \exp(0.3 \times i)$ with $i = 0, \ldots, 11$, where 0.3 corresponds to three times the coarsest calorimeter segmentation, $\Delta\eta = 0.1$. These χ distributions are measured in five dijet mass ranges with the expectation that low m_{jj} bins will be dominated by QCD processes and NP signals would be found in higher mass bins. The distributions are normalised to unit area, restricting the analysis to a shape comparison.

To facilitate an alternate approach to the study of dijet angular distributions, it is useful to define a single-parameter measure of isotropy as the fraction $F_\chi \equiv \frac{N_{\mathrm{central}}}{N_{\mathrm{total}}}$, where N_{total} is the number of events containing a dijet that passes all selection criteria, and N_{central} is the subset of these events in which the dijet enters a defined central region. It was found that $|y^*| < 0.6$, corresponding to $\chi < 3.32$, defines an optimal central region where many new processes would be expected to deviate from QCD predictions. This value corresponds to the upper boundary of the fourth bin in the χ distribution.

As in previous ATLAS studies [18], the current angular analyses make use of the $F_\chi(m_{jj})$ distribution, which consists of F_χ binned finely in m_{jj}:

$$F_\chi(m_{jj}) \equiv \frac{\mathrm{d}N_{\mathrm{central}}/\mathrm{d}m_{jj}}{\mathrm{d}N_{\mathrm{total}}/\mathrm{d}m_{jj}}, \tag{2.1}$$

using the same mass binning as the dijet mass analysis. This distribution is more sensitive to mass-dependent changes in the rate of centrally produced dijets than the χ distributions

JHEP01(2013)029

but is less sensitive to the detailed angular shape. The distribution of $F_\chi(m_{jj})$ in the central region defined above is similar to the m_{jj} spectrum, apart from an additional selection criterion on the boost of the system (as explained in section 4).

Dijet distributions from collision data are not corrected (unfolded) for detector resolution effects. Instead, the measured distributions are compared to theoretical predictions passed through detector simulation.

3 Jet calibration

The calorimeter cell structure of ATLAS is designed to follow the shower development of jets. Jets are reconstructed from topological clusters (topoclusters) [27] that group together cells based on their signal-to-noise ratio. The default jet algorithm in ATLAS is the anti-k_t algorithm [28, 29]. For the jet collection used in this analysis, the distance parameter of $R = 0.6$ is chosen. Jets are first calibrated at the electromagnetic scale (EM calibration), which accounts correctly for the energy deposited by electromagnetic showers but does not correct the scale for hadronic showers.

The hadronic calibration is applied in steps, using a combination of techniques based on Monte Carlo (MC) simulation and *in situ* measurements [30]. The first step is the pile-up correction which accounts for the additional energy due to collisions in the same bunch crossing as the signal event (in-time) or in nearby bunch crossings (out-of-time). Since the pile-up is a combination of these effects, the net correction may add or subtract energy from the jet. In the second step, the position of the jet origin is corrected for differences between the geometrical centre of the detector and the collision vertex. The third step is a jet energy correction using factors that are functions of the jet energy and pseudorapidity. These calibration factors are derived from MC simulation using a detailed description of the ATLAS detector geometry, which simulates the main detector response effects. The EM and hadronic calibration steps above are referred to collectively as the "EM+JES" scheme [31], which restores the hadronic jet response in MC to within 2%.

The level of agreement between data and MC simulation is further improved by the application of calibration steps based on *in situ* studies. First, the relative response in $|\eta|$ is equalised using an inter-calibration method obtained from balancing the transverse momenta of jets in dijet events [32]. Then the absolute energy response is brought into closer agreement with MC simulation by a combination of various techniques based on momentum balancing methods between photons or Z bosons and jets, and between high-momentum jets and a recoil system of low-momentum jets. This completes all the stages of the jet calibration.

The jet energy scale uncertainty is determined for jets with transverse momenta above 20 GeV and $|\eta| < 4.5$, based on the uncertainties of the *in situ* techniques and on systematic variations in MC simulations. For the most general case, covering all jet measurements made in ATLAS, the correlations among JES uncertainties are described by a set of 58 sources of systematic uncertainty (nuisance parameters). Uncertainties due to pile-up, jet flavour, and jet topology are described by five additional nuisance parameters. The total uncertainty from *in situ* techniques for central jets with a transverse momentum of 100 GeV is as low as 1% and rises to about 4% for jets with transverse momentum above 1 TeV.

JHEP01(2013)029

For the high-p_{T} dijet measurements made in the current analysis, the number of nuisance parameters is reduced to 14, while keeping a correlation matrix and total magnitude equivalent to the full configuration. This is achieved using a procedure that diagonalises the total covariance matrix found from *in situ* techniques, selects the largest eigenvalues as effective nuisance parameters, and groups the remaining parameters into one additional term.

The jet energy resolution is estimated both in data and in simulation using transverse momentum balance studies in dijet events, and they are found to be in good agreement [33]. Monte Carlo studies are used to assess the dijet mass resolution. Jets constructed from final state particles are compared to the calorimeter jets obtained after the same particles have been passed through full detector simulation. While the dijet mass resolution is found to be 10% at 0.20 TeV, it is reduced to approximately 5% within the range of high dijet masses considered in the current studies.

4 Event selection criteria

The triggers employed for this study select events that have at least one large (100 GeV or more) transverse energy deposition in the calorimeter. These triggers are also referred to as "single jet" triggers. To match the data rate to the processing and storage capacity available to ATLAS, a number of triggers with low-p_{T} thresholds were "prescaled". For these triggers only a preselected fraction of all events passing the threshold is recorded.

A single, unprescaled trigger is used for the dijet mass spectrum analysis. This single trigger is also used for the angular analyses at high dijet mass, but in addition several prescaled triggers are used at lower dijet masses. Each χ distribution is assigned a unique trigger, chosen to maximise the statistics, leading to a different effective luminosity for each distribution. Similar choices are made for the $F_{\chi}(m_{jj})$ distribution, assigning triggers to specific ranges of m_{jj} to maximise the statistics in each range. In all analyses, kinematic selection criteria ensure a trigger efficiency exceeding 99% for the events under consideration.

Events are required to have a primary collision vertex defined by two or more charged particle tracks. In the presence of additional pp interactions, the primary collision vertex chosen is the one with the largest scalar sum of p_{T}^2 for its associated tracks. In this analysis, the two highest-p_{T} jets are invariably associated with this largest sum of p_{T}^2 collection of tracks, which ensures that the correct collision vertex is used to reconstruct the dijet. Events are rejected if the data from the electromagnetic calorimeter have a topology as expected for non-collision background, or there is evidence of data corruption [34]. There must be at least two jets within $|y| < 4.4$ in the event, and all jets with $|y| \geq 4.4$ are discarded. The highest p_{T} jet is referred to as the "leading jet" (j_1), and the second highest as the "next-to-leading jet" (j_2). These two jets are collectively referred to as the "leading jets". Following the criteria in ref. [34], there must be no poorly measured jets with p_{T} greater than 30% of the p_{T} of the next-to-leading jet for events to be retained. Poorly measured jets correspond to energy depositions in regions where the energy measurement is known to be inaccurate. Furthermore, if either of the leading jets is not attributed to in-time energy depositions in the calorimeters, the event is rejected.

JHEP01(2013)029

A selection has been implemented to avoid a defect in the readout electronics of the electromagnetic calorimeter in the region from -0.1 to 1.5 in η, and from -0.9 to -0.5 in ϕ that occurred during part of the running period. The average response for jets in this region is 20% to 30% too low. For the m_{jj} analysis, events in the affected running period with jets near this region are rejected if such jets have a p_{T} greater than 30% of the next-to-leading jet p_{T}. This requirement removes 1% of the events. A similar rejection has been made for the angular analysis. In this case the complete η slice from -0.9 to -0.5 in ϕ is excluded in order to retain the shape of the distributions. The event reduction during run periods affected by the defect is 13%, and the overall reduction in the data set due to this effect is 4%.

Additional kinematic selection criteria are used to enrich the sample with events in the hard-scattering region of phase space. For the dijet mass analysis, events must satisfy $|y^*| < 0.6$ and $|\eta_{1,2}| < 2.8$ for the leading jets, and $m_{jj} > 850\,\mathrm{GeV}$.

For the angular analyses, events must satisfy $|y^*| < 1.7$ and $|y_B| < 1.1$, and $m_{jj} > 800\,\mathrm{GeV}$. The combined y^* and y_B criteria limit the rapidity range of the leading jets to $|y_{1,2}| < 2.8$. This $|y_B|$ selection does not affect events with dijet mass above 2.8 TeV since the phase space is kinematically constrained. The kinematic selection also restricts the minimum p_{T} of jets entering the analysis to 80 GeV. Since at lowest order $y_B = \frac{1}{2}\ln(\frac{x_1}{x_2})$ and $m_{jj}^2 = x_1\, x_2\, s$, with $x_{1,2}$ the parton momentum fractions of the colliding protons, the combined m_{jj} and y_B criteria result in limiting the effective $x_{1,2}$-ranges in the convolution of the matrix elements with the PDFs. The QCD matrix elements for dijet production lead to χ distributions that are approximately flat. Without the selection on y_B, the χ distributions predicted by QCD would have a slope becoming more pronounced for the lower m_{jj} bins. Restricting the $x_{1,2}$-ranges of the PDFs reduces this shape distortion, and also reduces the PDF and jet energy scale uncertainties associated with each χ bin of the final distribution.

5 Comparing the dijet mass spectrum to a smooth background

In the dijet mass analysis, a search for resonances in the m_{jj} spectrum is made by using a data-driven background estimate. The observed dijet mass distribution after all selection cuts is shown in figure 1. Also shown in the figure are the predictions for an excited quark for three different mass hypotheses [1, 2]. The m_{jj} spectrum is fit to a smooth functional form,

$$f(x) = p_1(1-x)^{p_2} x^{p_3+p_4 \ln x}, \tag{5.1}$$

where the p_i are fit parameters, and $x \equiv m_{jj}/\sqrt{s}$. In previous studies, ATLAS and other experiments [15, 17, 19, 22] have found this ansatz to provide a satisfactory fit to the QCD prediction of dijet production. The use of a full Monte Carlo QCD background prediction would introduce theoretical and systematic uncertainties of its own, whereas this smooth background form introduces only the uncertainties associated with its fit parameters. A feature of the functional form used in the fitting is that it allows for smooth background variations but does not accommodate localised excesses that could indicate the presence of NP signals. However, the effects of smooth deviations from QCD, such as contact

JHEP01(2013)029

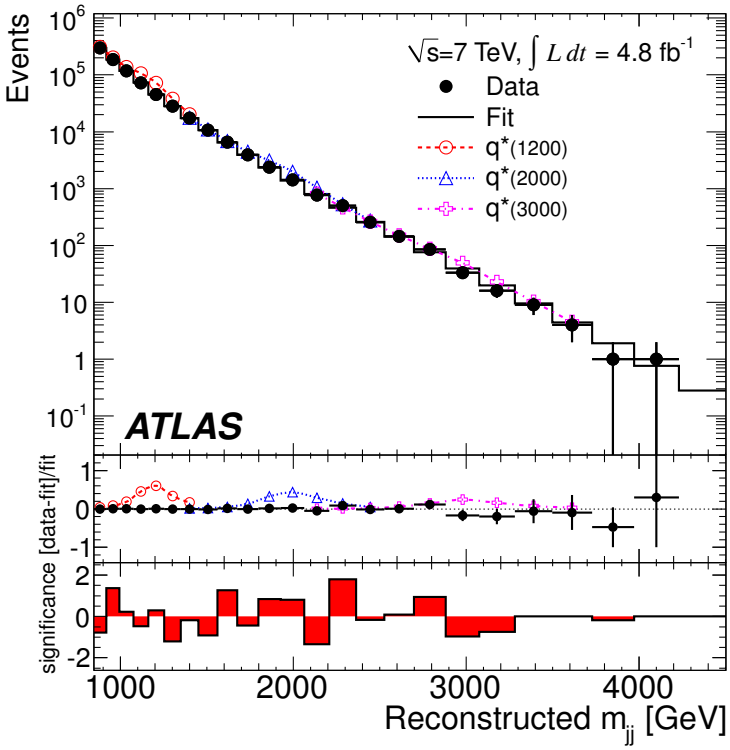

Figure 1. The reconstructed dijet mass distribution (filled points) fitted with a smooth functional form (solid line). Mass distribution predictions for three q^* masses are shown above the background. The middle part of figure shows the data minus the background fit, divided by the fit. The bin-by-bin significance of the data-background difference is shown in the lower panel.

interactions, could be absorbed by the background fitting function, and therefore the m_{jj} analysis is used only to search for resonant effects.

The χ^2-value of the fit is 17.7 for 22 degrees of freedom, and the reduced χ^2 is 0.80. The middle part of figure 1 shows the data minus the background fit, divided by the fit. The lower part of figure 1 shows the significance, in standard deviations, of the difference between the data and the fit in each bin. The significance is calculated taking only statistical uncertainties into account, and assuming that the data follow a Poisson distribution. For each bin a p-value is determined by assessing the probability of the background fluctuating higher than the observed excess or lower than the observed deficit. This p-value is transformed to a significance in terms of an equivalent number of standard deviations (the z-value) [35]. Where there is an excess (deficit) in data in a given bin, the significance is plotted as positive (negative).[2] To test the degree of consistency between the data and the fitted background, the p-value of the fit is determined by calculating the χ^2-value from the data and comparing this result to the χ^2 distribution obtained from pseudo-experiments

[2]In mass bins with small expected number of events, where the observed number of events is similar to the expectation, the Poisson probability of a fluctuation at least as high (low) as the observed excess (deficit) can be greater than 50%, as a result of the asymmetry of the Poisson distribution. Since these bins have too few events for the significance to be meaningful, the bars are not drawn for them.

JHEP01(2013)029

drawn from the background fit, as described in a previous publication [22]. The resulting p-value is 0.73, showing that there is good agreement between the data and the fit.

As a more sensitive test, the BumpHunter algorithm [36, 37] is used to establish the presence or absence of a resonance in the dijet mass spectrum, as described in greater detail in previous publications [22, 23]. Starting with a two-bin window, the algorithm increases the signal window and shifts its location until all possible bin ranges, up to half the mass range spanned by the data, have been tested. The most significant departure from the smooth spectrum ("bump") is defined by the set of bins that have the smallest probability of arising from a background fluctuation assuming Poisson statistics.

The BumpHunter algorithm accounts for the so-called "look-elsewhere effect" [38], by performing a series of pseudo-experiments drawn from the background estimate to determine the probability that random fluctuations in the background-only hypothesis would create an excess anywhere in the spectrum at least as significant as the one observed. Furthermore, to prevent any NP signal from biasing the background estimate, if the most significant local excess from the background fit has a p-value smaller than 0.01, this region is excluded and a new background fit is performed. No such exclusion is needed for this data set.

The most significant discrepancy identified by the BumpHunter algorithm in the observed dijet mass distribution in figure 1 is a four-bin excess in the interval 2.21 TeV to 2.88 TeV. The probability of observing such an excess or larger somewhere in the mass spectrum for a background-only hypothesis is 0.69. This test shows no evidence for a resonance signal in the m_{jj} spectrum.

6 QCD predictions for dijet angular distributions

In the dijet angular analyses, the QCD prediction is based on MC generation of event samples which cover the kinematic range in χ and m_{jj} spanned by the selected dijet events. The QCD hard scattering interactions are simulated using the Pythia 6 [39] event generator with the ATLAS AUET2B LO** tune [40] which uses the MRSTMCal [41] modified leading-order (LO) parton distribution functions (PDFs).

To incorporate detector effects, these QCD events are passed through a fast detector simulation, ATLFAST 2.0 [42], which employs FastCaloSim [43] for the simulation of electromagnetic and hadronic showers in the calorimeter. Comparisons with detailed simulations of the ATLAS detector [44, 45] using the Geant4 package [45] show no differences in the angular distributions exceeding 5%.

To simulate in-time pile-up, separate samples of inelastic interactions are generated using Pythia 8 [46], and these samples are passed through the full detector simulation. To simulate QCD events in the presence of pile-up, hard scattering events are overlaid with μ inelastic interactions, where μ is Poisson distributed, and the distribution of $\langle\mu\rangle$ is chosen to match the distribution of average number of interactions per bunch crossings in data. The combined MC events, containing one hard interaction and several soft interactions, are then reconstructed in the same way as collision data and are subjected to the same event selection criteria as applied to collision data.

JHEP01(2013)029

Bin-by-bin correction factors (K-factors) are applied to the angular distributions derived from MC calculations to account for NLO contributions. These K-factors are derived from dedicated MC samples and are defined as the ratio NLO_{ME}/PYT_{SHOW}. The NLO_{ME} sample is produced using NLO matrix elements in NLOJET++ [47–49] with the NLO PDF from CT10 [50]. The PYT_{SHOW} sample is produced with the Pythia 6 generator restricted to leading-order matrix elements and with parton showering but with non-perturbative effects turned off. This sample also uses the AUET2B LO** tune.

The angular distributions generated with the full Pythia simulation include various non-perturbative effects including hadronisation, underlying event, and primordial $k_\perp$. The K-factors defined above are designed to retain these effects while adjusting for differences in the treatment of perturbative effects. The full Pythia predictions of angular distributions are multiplied by these bin-wise K-factors to obtain reshaped spectra that include corrections originating from NLO matrix elements. K-factors are applied to χ distributions before normalising them to unit area. The K-factors change the normalised χ distributions by 2% at low dijet mass, by as much as 11% in the highest dijet mass bins, and the effect is largest at low χ. The K-factors for $F_\chi(m_{jj})$ are close to unity for dijet masses of around 1 TeV, but increase with dijet mass, and are as large as 20% for dijet masses of 4 TeV. Electroweak corrections are not included in the theoretical predictions [51].

7 Comparing χ distributions to QCD predictions

The observed χ distributions normalised to unit area are shown in figure 2 for several m_{jj} bins, defined by boundaries at 800, 1200, 1600, 2000, and 2600 GeV. The highest bin includes all dijet events with $m_{jj} > 2.6$ TeV. The dijet mass bins are chosen to ensure sufficient entries in each mass bin. From the lowest dijet mass bin to the highest bin, the number of events are: 13642, 4132, 35250, 28462, 2706, and the corresponding integrated luminosities are 5.6 pb^{-1}, 19.2 pb^{-1}, 1.2 fb^{-1}, 4.8 fb^{-1} and 4.8 fb^{-1}. The yield for all $m_{jj} < 2000$ GeV is reduced due to the usage of prescaled triggers, and for $m_{jj} > 2000$ GeV by the falling cross section.

The χ distributions are compared to the predictions from QCD, which include all systematic uncertainties, and the signal predictions of one particular NP model, a quantum black hole (QBH) scenario with a quantum gravity mass scale of 4.0 TeV and six extra dimensions [7, 8].

Pseudo-experiments are used to convolve statistical, systematic and theoretical uncertainties on the QCD predictions, as has been done in previous studies of this type [18]. The primary sources of theoretical uncertainty are NLO QCD renormalisation and factorisation scales, and PDF uncertainties. The QCD scales are varied by a factor of two independently around their nominal values, which are set to the mean p_{T} of the leading jets, while the PDF uncertainties are determined using CT10 NLO PDF error sets [52]. The resulting bin-wise uncertainties for the cross-section normalised χ distributions can be as high as 8% for the combined NLO QCD scale variations and are typically below 1% for the PDF uncertainties. These theoretical uncertainties are convolved with the JES uncertainty and applied to all MC angular distributions. Other experimental uncertainties such as those

JHEP01(2013)029

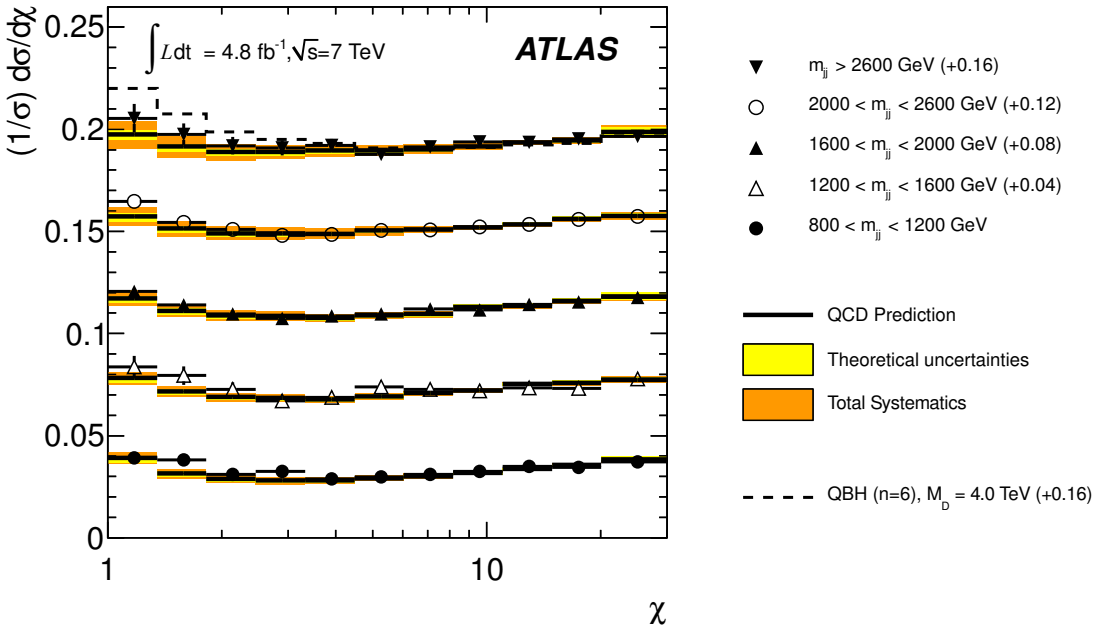

Figure 2. The χ distributions for all dijet mass bins. The QCD predictions are shown with theoretical and total systematic uncertainties (bands), as well as the data with statistical uncertainties. The dashed line is the prediction for a QBH signal for $M_D = 4.0\,\text{TeV}$ and $n = 6$ in the highest mass bin. The distributions have been offset by the amount shown in the legend to aid in visually comparing the shapes in each mass bin.

due to pile-up and to the jet energy and angular resolutions have been investigated and found to be negligible. The JES uncertainties are largest at low χ and are as small as 5% for the lowest dijet mass bin but increase to above 15% for the highest bin. Variations based on the resulting systematic uncertainties are used in generating statistical ensembles for the estimation of p-values when comparing QCD predictions to data.

A statistical analysis is performed on each of the five χ distributions to test the overall consistency between data and QCD predictions. A binned log-likelihood is calculated for each distribution assuming that the sample consists only of QCD dijet production. The expected distribution of this likelihood is then determined using pseudo-experiments drawn from the QCD MC sample and convolved with the systematic uncertainties as discussed above. Finally the p-value is defined as the probability of obtaining a log-likelihood value less than the value observed in data.

The p-values determined from the observed likelihoods are shown in table 1. These indicate that there is no statistically significant evidence for new phenomena in the χ distributions, and that these distributions are in reasonable agreement with QCD predictions.

As with the dijet resonance analysis, the BumpHunter algorithm is applied to the five χ distributions separately, in this case to test for the presence of features that might indicate disagreement with the QCD prediction. The results are shown in table 1. In this particular application, the BumpHunter is required to start from the first χ bin, and the excess must be at least three bins wide. For each of the bin combinations, the binomial p-value for observing the data given the QCD-background-only hypothesis is calculated. The bin sequence with the smallest binomial p-value is listed in table 1. Statistical and

JHEP01(2013)029

m_{jj} bin [GeV]	LL p-value	BH Discrep	BH p-value
800–1200	0.23	bin 1–9	0.17
1200–1600	0.31	bin 1–7	0.20
1600–2000	0.56	bin 1–7	0.37
2000–2600	0.74	bin 1–3	0.38
> 2600	0.83	bin 1–10	0.37

Table 1. Comparing χ distributions to QCD predictions. The abbreviations in the first line of the table stand for "log-likelihood" (LL), and "BumpHunter" (BH). The second line labels the "p-values" (p-value) and the "most discrepant region" (Discrep).

systematic uncertainties, and look-elsewhere effects, are included using pseudo-experiments drawn from the QCD background. For each of the pseudo-experiments the most discrepant bin combination is found and its p-value is used to construct the expected binomial p-value distribution. The final BumpHunter p-value is then defined as the probability of finding a binomial p-value as extreme as the one observed in data. The p-values listed in the last column of table 1 indicate that the data are consistent with the QCD prediction in all five mass bins.

In addition, the BumpHunter algorithm is applied to all χ distributions at once, which increases the effect of the correction for the look-elsewhere effect. The most discrepant region in all distributions is in bins 1–9 of the 800–1200 GeV mass distribution. The resulting p-value, including the look-elsewhere effect, is now 0.43, again indicating good agreement with QCD predictions.

8 Comparing the $F_\chi(m_{jj})$ distribution to the QCD prediction

The observed $F_\chi(m_{jj})$ data distribution is shown in figure 3, where it is compared to the QCD prediction, which includes all systematic uncertainties. Also shown in the figure is the expected behaviour of $F_\chi(m_{jj})$ if a contact interaction with the compositeness scale $\Lambda = 7.5$ TeV were present [53, 54]. Furthermore the predictions for an excited quark with a mass of 2.5 TeV and a QBH signal with $M_D = 4.0$ TeV are shown. The blue vertical line at 1.8 TeV included in figure 3 indicates the mass boundary above which the search phase of the analysis is performed, as explained below.

The observed $F_\chi(m_{jj})$ distribution is obtained by forming the finely-binned m_{jj} distributions for N_{central} and N_{total} — the "numerator" and "denominator" distributions of $F_\chi(m_{jj})$ — separately and taking the ratio. The handling of systematic uncertainties, including JES, PDF and scale uncertainties, uses a procedure similar to that for the χ distributions.

Two statistical tests are applied to the high-mass region to determine whether the data are compatible with the QCD prediction. The first test uses a binned likelihood, which includes the systematic uncertainties, and is constructed assuming the presence of QCD

JHEP01(2013)029

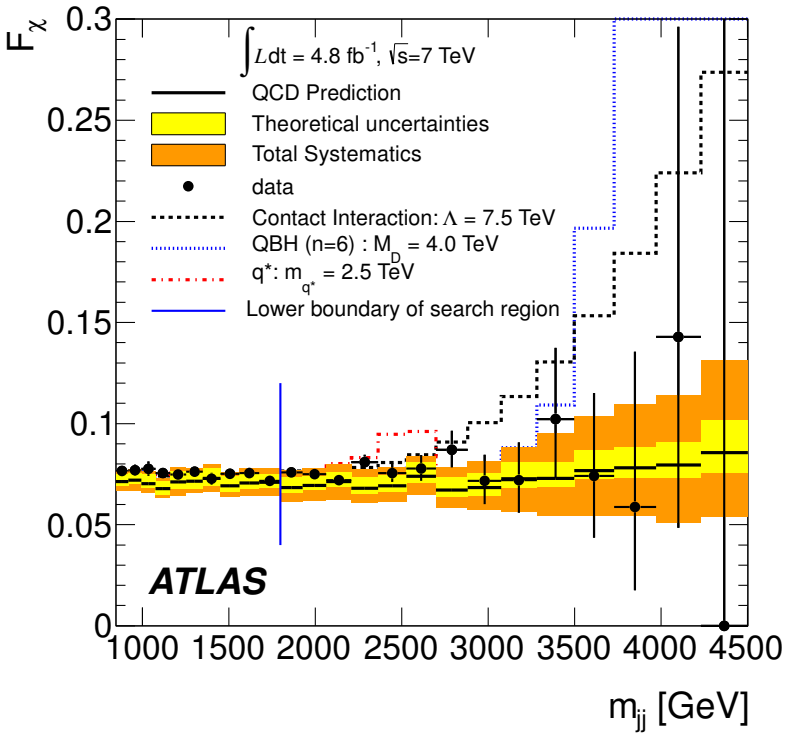

Figure 3. The $F_\chi(m_{jj})$ distribution in m_{jj}. The QCD prediction is shown with theoretical and total systematic uncertainties (bands), and data (black points) with statistical uncertainties. The blue vertical line indicates the lower boundary of the search region for new phenomena. Various expected new physics signals are shown: a contact interaction with $\Lambda = 7.5\,\text{TeV}$, an excited quark with mass 2.5 TeV and a QBH signal with $M_D = 4.0\,\text{TeV}$.

processes only. The p-value calculated from this likelihood is 0.38, indicating that these data are in agreement with the QCD prediction.

The second test consists of applying the BumpHunter and TailHunter algorithms [36, 37] to the $F_\chi(m_{jj})$ distributions, including systematic uncertainties and assuming binomial statistics. For this test only data with dijet masses above 1.8 TeV, associated with the single unprescaled trigger, are used to obtain a high sensitivity at high mass and to avoid diluting the test with the large number of low-mass bins. The test scans the data using windows of varying widths and identifies the window with the largest excess of events with respect to the background. The BumpHunter finds the most discrepant interval to be from 1.80 TeV to 2.88 TeV, with a p-value of 0.20. The TailHunter finds the most discrepant interval to be from 1.80 TeV onwards, with a p-value of 0.21. The p-values indicate that there is no significant excess in the data .

9 Simulation of hypothetical new phenomena

In the absence of any significant signals indicating the presence of phenomena beyond QCD, Bayesian 95% credibility level (CL) limits are determined for a number of NP hypotheses. The following models have been described in detail in previous ATLAS dijet studies [17,

JHEP01(2013)029

18, 22, 23]: quark contact interactions (CI) [53, 54], excited quarks (q^*) [1, 2], colour octet scalars (s8) [6], and quantum black holes (QBH) [7, 8]. Two models of new phenomena are added to the current analysis: heavy W bosons (W') with SM couplings [55–57], and string resonances (SR) [9–12]. Contact interactions and QBH appear as slowly rising effects in m_{jj}, while the other hypotheses produce localised excesses.

A number of these NP models are available in the Pythia 6 event generator. In these cases, the corresponding MC samples are generated using the AUET2B LO** tune and the MRSTMCal PDF. For NP models provided by other event generators, with other PDFs, partons originating from the initial two-parton interaction are used as input to Pythia which performs parton showering and the remaining event generation steps. In all cases, the renormalisation and factorisation scales are set to the mean p_{T} of the leading jets.

The quark contact interaction, CI, is used to model the appearance of kinematic properties that characterise quark compositeness. In the current analysis, only destructive interference is studied, but constructive interference is expected to give less conservative limits. Pythia 6 is used to create MC event samples for distinct values of the compositeness scale, Λ.

Excited quarks, q^* , a possible manifestation of quark compositeness, are also simulated in all decay modes with Pythia 6 for selected values of the q^* mass. Excited quarks are assumed to decay to common quarks via standard model couplings, leading to gluon emission approximately 83% of the time. Recent studies comparing this benchmark model to the same excited quark model in Pythia 8 show that the q^* m_{jj} distribution in Pythia 8 is significantly broader than that in Pythia 6. The Pythia authors have identified a long-standing misapplication of QCD p_{T}-ordered final state radiation (FSR) vetoing in Pythia 6, which is resolved in Pythia 8. The q^* m_{jj} distributions from Pythia 6 can be brought into close correspondence with Pythia 8 by setting the Pythia 6 MSTJ(47) parameter to zero, restoring the correct behaviour for final state radiation. The resulting widening of the peak affects the search sensitivity and exclusion limits. The q^* MC samples used in the current studies are generated using both the default and corrected Pythia 6 settings, to determine the impact on the q^* exclusion limit.

The colour octet scalar model, s8, is a typical example of possible exotic coloured resonances decaying to two gluons. MadGraph 5 [58] with the CTEQ6L1 PDF [59] is employed to generate parton-level event samples at leading-order approximation for a selection of s8 masses, which are used as input to Pythia 6.

A model for quantum black holes, QBH, that decay to two jets is simulated using BlackMax [60] with the CT10 PDF to produce a simple two-body final state scenario of quantum gravitational effects at the reduced Planck Scale M_D, with $n = 6$ extra spatial dimensions. The QBH model is used as a benchmark to represent any quantum gravitational effect that produces events containing dijets. Event samples for selected values of M_D are used as input to Pythia for further processing.

The first new NP phenomenon used in the current dijet analysis, the production of heavy charged gauge bosons, W', has been sought in events containing a charged lepton (electron or muon) and a neutrino [56, 57], but no evidence has been found. In the current studies, dijet events are searched for the decays of W' to $q\bar{q}'$. The specific model used in

JHEP01(2013)029

this study [55] assumes that the W' has V-A SM couplings but does not include interference between the W' and the W. The W' signal sample is generated with the Pythia 6 event generator. Instead of the LO cross section values, the NNLO electroweak-corrected cross section values [57, 61–63] calculated using the MSTW2008 PDF [64], are used in this analysis. For a given W' mass, the width of the resonance in m_{jj} is very similar to that of the q^*, and the angular distribution peaks at low χ. The limit analysis for this W' model includes the branching ratio to the chosen $q\bar{q}'$ final state and, for each simulated mass, this fraction is taken from Pythia 6.

The second new NP model considered, string resonances (SR), results from excitations of quarks and gluons at the string level [9–12]. The dominant decay mode is to qg, and the SR model described in ref. [11] is implemented in the CalcHEP generator [65] with the MRSTMCal PDF. As with other models, MC samples are created for selected values of the mass parameter, m_{SR}, by passing the CalcHEP output at parton level to Pythia 6.

All MC signal samples are passed through fast detector simulation using ATLFAST 2.0, except for string resonances, which are fully simulated using Geant4.

10 Limits on new resonant phenomena from the m_{jj} distribution

For each NP process under study, Monte Carlo samples have been simulated at a number of selected mass points, m_{NP}. The Bayesian method documented in ref. [22] is applied to data at these same mass points to set a 95% CL limit on the cross section times acceptance, $\sigma \times \mathcal{A}$, for the NP signal as a function of m_{NP}, using a prior constant in signal strength. The limit on $\sigma \times \mathcal{A}$ from data is interpolated between mass points to create a continuous curve in m_{jj}. The exclusion limit on the mass (or energy scale) of the given NP signal occurs at the value of m_{jj} where the limit on $\sigma \times \mathcal{A}$ from data is the same as the theoretical value, which is derived by interpolation between the generated mass values.

This form of analysis is applicable to all resonant phenomena where the NP couplings are strong compared to the scale of perturbative QCD at the signal mass, so that interference with QCD terms can be neglected. The acceptance calculation includes all reconstruction steps and analysis cuts described in section 4. For all resonant models except for the W', all decay modes have been simulated so that the branching ratio into dijets is implicitly included in the acceptance through the analysis selection. For the W' model, only dijet final states have been simulated, and the branching ratio is included in the cross section instead of in the acceptance.

The effects of systematic uncertainties due to luminosity, acceptance, and jet energy scale are included. The luminosity uncertainty for the 2011 data is 3.9% [24] and is combined in quadrature with the acceptance uncertainty. The correlated systematic uncertainties corresponding to the 14 JES nuisance parameters are added in quadrature and represented by a single nuisance parameter which shifts the resonance mass peaks by less than 4%. The background parameterisation uncertainty is taken from the fit results, as described in ref. [22]. The effect of the jet energy resolution uncertainty is found to be negligible.

These uncertainties are incorporated into the fit by varying all sources according to Gaussian probability distributions and convolving them with the posterior probability dis-

JHEP01(2013)029

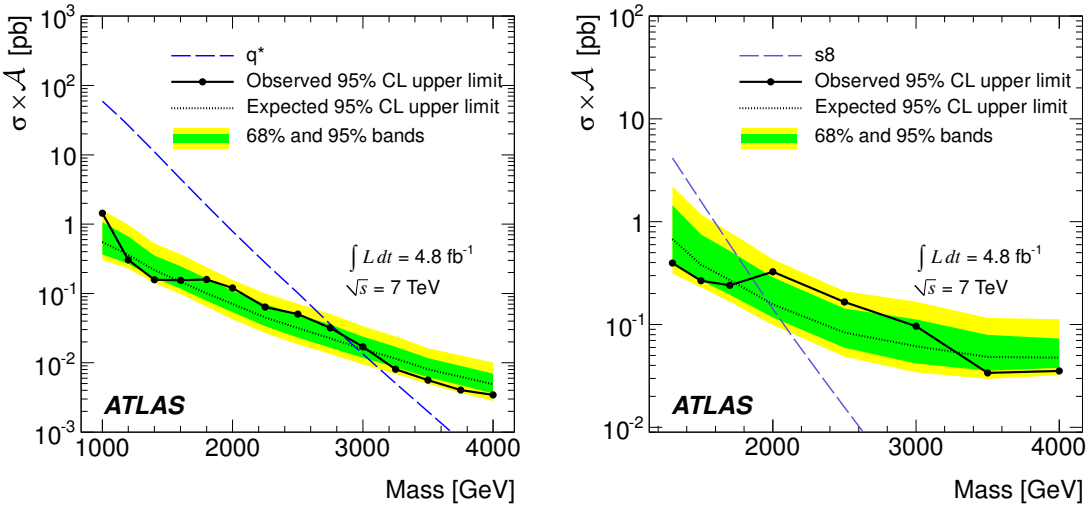

(a) Excited-quark model.

(b) Colour scalar octet model.

Figure 4. The 95% CL upper limits on $\sigma \times \mathcal{A}$ as a function of particle mass (black filled circles) using m_{jj}. The black dotted curve shows the 95% CL upper limit expected in the absence of any resonance signal, and the green and yellow bands represent the 68% and 95% contours of the expected limit, respectively. Theoretical predictions of $\sigma \times \mathcal{A}$ are shown (dashed) in (a) for excited quarks, and in (b) for colour octet scalars. For a given NP model, the observed (expected) limit occurs at the crossing of the dashed $\sigma \times \mathcal{A}$ curve with the observed (expected) 95% CL upper limit curve.

tribution. Credibility intervals are then calculated numerically from the resulting convolutions. No uncertainties are associated with the theoretical model, as in each case the NP model is a benchmark that incorporates a specific choice of model parameters, PDF set, and MC tune. Previous ATLAS studies using the q^* theoretical prediction [22] showed that the variation among three different choices of MC tune and PDF set was less than 4% for the expected limits.

The resulting limits for excited quarks, based on the corrected Pythia 6 samples (as explained in section 9), are shown in figure 4(a). The acceptance $\mathcal{A}$ ranges from 40% to 51% for m_{q^*} between 1.2 TeV and 4.0 TeV, and is never lower than 46% for masses above 1.4 TeV. The largest reduction in acceptance arises from the rapidity selection criteria. The expected lower mass limit at 95% CL for q^* is 2.94 TeV, and the observed limit is 2.83 TeV. For comparison, this limit has also been determined using Pythia 6 samples with the default q^* settings, leading to narrower mass peaks. The expected limit determined from these MC samples is 0.1 TeV higher than the limit based on the corrected samples. This shift is an approximate indicator of the fractional correction that is expected when comparing the current ATLAS results to all previous analyses that found q^* mass limits using Pythia 6 and p_{T}-ordered final state radiation without corrections, including all previous ATLAS results.

The limits for colour octet scalars are shown in figure 4(b). The expected mass limit at 95% CL is 1.97 TeV, and the observed limit is 1.86 TeV. For this model the acceptance values vary between 34% and 48% for masses between 1.3 TeV and 4.0 TeV.

JHEP01(2013)029

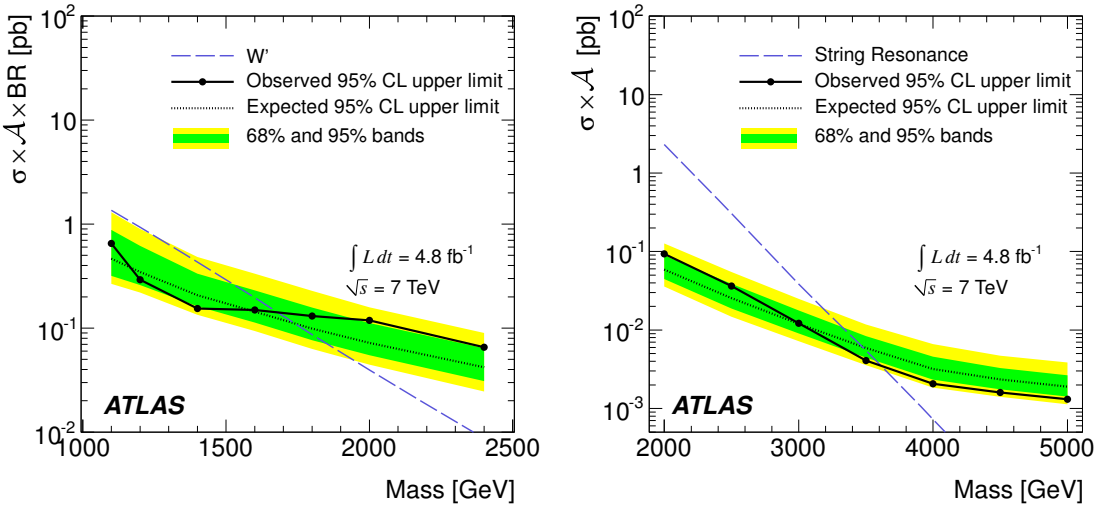

(a) Heavy charged gauge bosons, W'.

(b) String resonances, SR.

Figure 5. In (a), 95% CL upper limits on $\sigma \times \mathcal{A} \times$ BR as a function of particle mass (black filled circles) from m_{jj} analysis are shown for heavy gauge bosons, W'. The black dotted curve shows the 95% CL upper limit expected in the absence of any resonance signal, and the green and yellow bands represent the 68% and 95% contours of the expected limit, respectively. The observed (expected) limit occurs at the crossing of the dashed theoretical $\sigma \times \mathcal{A} \times$ BR curve with the observed (expected) 95% CL upper limit curve. In (b), 95% CL upper limits on $\sigma \times \mathcal{A}$ are shown for string resonances, SR, with the equivalent set of contours for this model, and the same method of limit determination.

The limits for heavy charged gauge bosons, W', are shown in figure 5(a). For this model, only final states with dijets have been simulated. The branching ratio, BR, to the studied $q\bar{q}'$ final state varies little with mass and is 0.75 for $m_{W'}$ values of 1.1 TeV to 3.6 TeV, and the acceptance ranges from 29% to 36%. The expected mass limit at 95% CL is 1.74 TeV, and the observed limit is 1.68 TeV. This is the first time that an ATLAS limit on W' production is set using the dijet mass distribution. Searches for leptonic decays of the W' are however expected to be more sensitive.

The W' hypothesis used in the current study assumes SM couplings to quarks. If a similar model were to predict stronger couplings, for example, figure 5(a) could be used to estimate the new mass limit by shifting the theoretical curve upward by the ratio of the squared couplings. Alternately, the current limit on W' decaying to dijets could be of interest for comparison with leptophobic W' models, where all final states would be hadronic [66–69].

The limits for string resonances are shown in figure 5(b). The SR acceptance ranges from 45% to 48% for masses varying from 2.0 TeV to 5.0 TeV. The expected mass limit at 95% CL is 3.47 TeV, and the observed limit is 3.61 TeV.

Tables with acceptance values and limits for all models discussed here can be found in appendix A.

JHEP01(2013)029

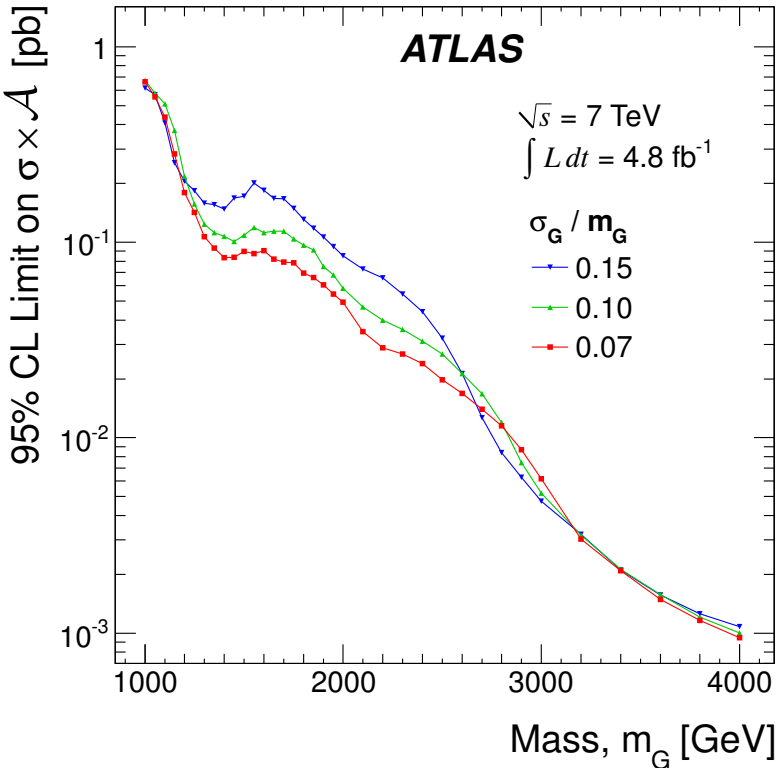

Figure 6. The 95% CL upper limits on $\sigma \times \mathcal{A}$ for a simple Gaussian resonance decaying to dijets as a function of the mean mass, m_{G}, for three values of $\sigma_{\mathrm{G}}/m_{\mathrm{G}}$, taking into account both statistical and systematic uncertainties.

11 Model-independent limits on dijet resonance production

As in previous dijet resonance analyses, limits on dijet resonance production are determined here using a Gaussian resonance shape hypothesis. Limits are set for a collection of hypothetical signals that are assumed to be Gaussian-distributed in m_{jj} with means (m_{G}) ranging from 1.0 TeV to 4.0 TeV and with standard deviations (σ_{G}) from 7% to 15% of the mean.

Systematic uncertainties are treated using the same methods as applied in the model-dependent limit setting described above. The only difference between the Gaussian analysis and the standard analysis is that the decay of the dijet final state is not simulated. In place of this, it is assumed that the dijet signal mass distribution is Gaussian in shape, and the JES uncertainty is modelled as an uncertainty of 4% in the central value of the Gaussian signal. This approach has been validated by shifting the energy of all jets in Pythia 6 signal templates by their JES uncertainty and evaluating the relative shift of the mass peak.

The resulting limits on $\sigma \times \mathcal{A}$ for the Gaussian template model are shown in figure 6 and detailed in table 2. These results may be utilised to set limits on NP models beyond those considered in the current studies, under the condition that their signal shape approaches a Gaussian distribution after applying the kinematic selection criteria on y^*, m_{jj} and η of the

JHEP01(2013)029

leading jets (section 4). The acceptance should include the branching ratio of the particle decaying into dijets and the physics selection efficiency. The ATLAS m_{jj} resolution is about 5%, hence NP models with a width smaller than 7% should be compared to the 7% column of table 2. Models with a greater width should use the column that best matches their width. A detailed description of the recommended procedure, including the treatment of detector resolution effects, is given in ref. [23].

12 Limits on CI and QBH from the χ distributions

The χ distribution in the highest mass bin of figure 2 is used to set 95% CL limits on two NP hypotheses, CI and QBH.

In the contact interaction analysis, four MC samples of QCD production modified by a contact interaction are created for values of Λ ranging from 4.0 TeV to 10.0 TeV. For the CI distributions, QCD K-factors are applied to the QCD-only component of the cross section, as follows: before normalising the χ-distributions to unit area, the LO QCD part of the cross section, determined from a QCD-only simulation sample, is replaced by the QCD cross section corrected for NLO effects.

Using the QCD distribution and the finite set of MC CI distributions, each χ-bin is fit as function of Λ against a four-parameter interpolation function,[3] allowing for a smooth integration of the posterior probability density functions over Λ. From the signal fits, a posterior probability density is constructed as a function of Λ. The systematic uncertainties described in section 7 are convolved with the posterior distribution through pseudo-experiments drawn from the NP hypotheses. For the expected limit, pseudo-experiments are performed on the QCD background and used as pseudo-data.

This analysis sets a 95% CL lower limit on Λ at 7.6 TeV with an expected limit of 7.7 TeV. The observed posterior probability density function is shown in figure 7.

To test the sensitivity of the CI limit to the choice of prior, this analysis is repeated for a constant prior in $1/\Lambda^2$, which has been used in previous publications. As anticipated, the expected limit is less conservative, increasing by 0.40 TeV. Since the constant prior in $1/\Lambda^4$ more accurately follows the cross section predicted for CI, the $1/\Lambda^2$ result is not reported in the final results of the current studies.

The second model is QBH with $n = 6$ and with a constant prior in $1/M_D^4$, which is for $n = 6$ proportional to the cross section. Similarly to what is done for CI, the QCD sample, together with a set of eleven QBH samples with M_D ranging from 2.0 TeV to 6.0 TeV, is fit to the same smooth function in every χ-bin to enable integration of the posterior probability density functions over M_D. The expected and observed 95% CL lower limits on M_D are 4.20 TeV and 4.11 TeV, respectively.

13 Limits on new resonant phenomena from the $F_\chi(m_{jj})$ distribution

The Bayesian approach employed to set exclusion limits on new resonant phenomena with the dijet mass spectrum may be applied to the $F_\chi(m_{jj})$ distribution (see figure 3), pro-

[3] The fitting function is $f(x) = p_4 / \left[\exp\left(p_1\left(p_2 - \log(x)\right)\right) + 1\right] + p_3$, $x = 1/\Lambda^2$.

m_{G} [GeV]	Observed 95% CL upper limits on $\sigma \times \mathcal{A}$ [pb]		
	$\sigma_{\mathrm{G}}/m_{\mathrm{G}} = 7\%$	$\sigma_{\mathrm{G}}/m_{\mathrm{G}} = 10\%$	$\sigma_{\mathrm{G}}/m_{\mathrm{G}} = 15\%$
1000	0.66	0.67	0.61
1050	0.56	0.58	0.57
1100	0.44	0.51	0.41
1150	0.28	0.37	0.26
1200	0.18	0.22	0.21
1250	0.14	0.16	0.18
1300	0.11	0.12	0.16
1350	0.093	0.11	0.16
1400	0.083	0.11	0.15
1450	0.084	0.10	0.17
1500	0.090	0.11	0.17
1550	0.087	0.12	0.20
1600	0.090	0.11	0.18
1650	0.082	0.11	0.17
1700	0.079	0.11	0.17
1750	0.078	0.10	0.15
1800	0.069	0.097	0.13
1850	0.066	0.091	0.12
1900	0.061	0.075	0.11
1950	0.054	0.068	0.095
2000	0.049	0.058	0.085
2100	0.035	0.047	0.073
2200	0.029	0.040	0.066
2300	0.027	0.036	0.054
2400	0.024	0.031	0.044
2500	0.020	0.027	0.032
2600	0.017	0.021	0.021
2700	0.014	0.017	0.013
2800	0.012	0.012	0.0084
2900	0.0087	0.0075	0.0063
3000	0.0062	0.0052	0.0047
3200	0.0030	0.0032	0.0032
3400	0.0021	0.0021	0.0021
3600	0.0015	0.0016	0.0016
3800	0.0012	0.0012	0.0013
4000	0.0010	0.0010	0.0011

Table 2. The 95% CL upper limit on $\sigma \times \mathcal{A}$ [pb] for the Gaussian model. The symbols m_{G} and σ_{G} are, respectively, the mean mass and standard deviation of the Gaussian.

JHEP01(2013)029

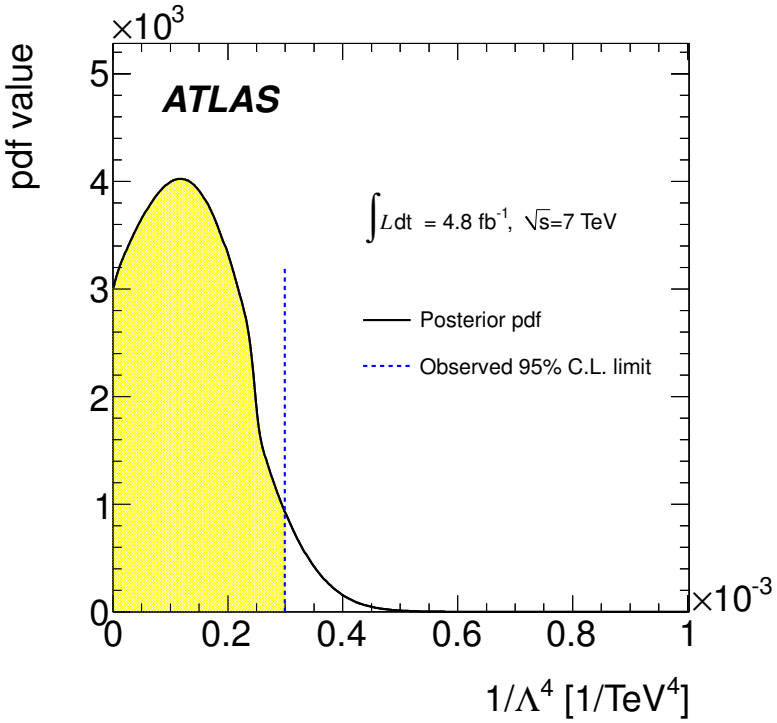

Figure 7. Observed posterior probability density function as function of $1/\Lambda^4$ for the CI model. The coloured area shows the 95% area, and the blue dashed line denotes the 95% CL limit.

vided that the NP models under consideration do not include interference with QCD. Unlike the m_{jj} resonance analysis, the background prediction is based on the QCD MC samples processed through detector simulation and corrected for NLO effects. The likelihood is constructed from two m_{jj} distributions and their associated uncertainties, one distribution being the numerator spectrum of the $F_\chi(m_{jj})$ distribution and the other being the denominator. Here too, pseudo-experiments are used to convolve all systematic uncertainties, which in this case include the JES uncertainties, and the PDF and scale uncertainties associated with the QCD prediction.

Figure 8 shows the limits expected and observed from data on the production cross section σ times the acceptance $\mathcal{A}$, along with theoretical predictions for the QBH model [7, 8], for n ranging from two to seven. For this model, generator-level studies have shown that the acceptance does not depend on the number of extra dimensions within this range. Therefore only the QBH MC sample for $n = 6$ has been processed through the ATLFAST 2.0 detector simulation, and the acceptance calculated from this sample is used for all values of n. The acceptance is close to 90% for all M_D values. The resulting 95% CL exclusion limits for the number of extra dimensions n ranging from 2 to 7 are shown in table 3.

The same analysis is applied to detect resonances in $F_\chi(m_{jj})$ due to excited quarks. With an acceptance close to 90% for all masses this analysis sets a 95% CL lower limit on m_{q^*} at 2.75 TeV with an expected limit of 2.85 TeV.

JHEP01(2013)029

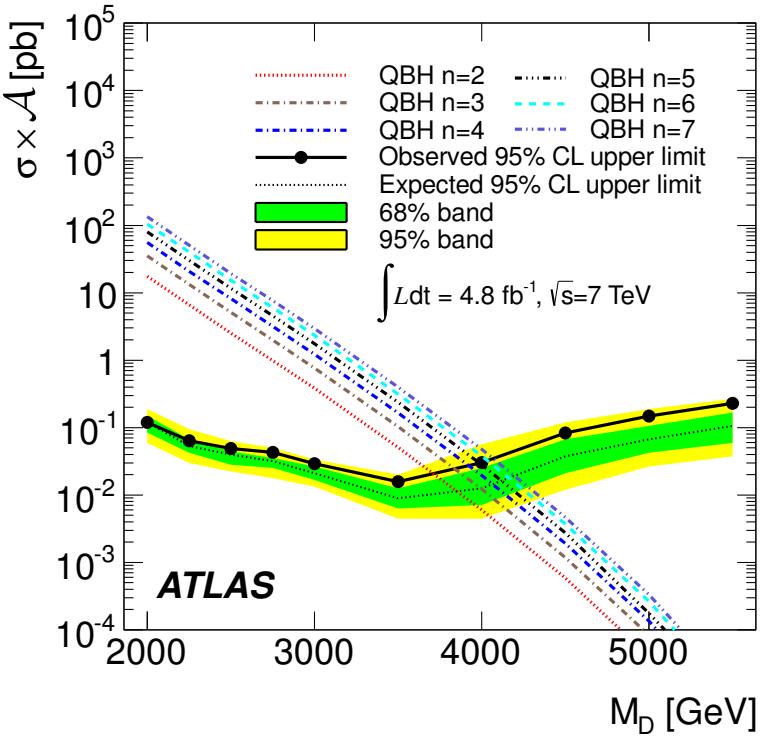

Figure 8. The 95% CL upper limits on $\sigma \times \mathcal{A}$ as function of the reduced Planck mass M_D of the QBH model using $F_\chi(m_{jj})$ (black filled circles). The black dotted curve shows the 95% CL upper limit expected from Monte Carlo, and the green and yellow bands represent the 68% and 95% contours of the expected limit, respectively. Theoretical predictions of $\sigma \times \mathcal{A}$ are shown for various numbers of extra dimensions.

n extra dimensions	Expected limit [TeV]	Observed limit [TeV]
2	3.85	3.71
3	3.99	3.84
4	4.07	3.92
5	4.12	3.99
6	4.16	4.03
7	4.19	4.07

Table 3. Lower limits at 95% CL on M_D of the QBH model with $n = 2$ to 7 extra dimensions.

14 Limits on CI from the $F_\chi(m_{jj})$ distribution

As was done previously with the ATLAS 2010 data sample [22], the $F_\chi(m_{jj})$ distribution (see figure 3) is used in the current study to set limits on quark contact interactions.

The procedure is very similar to the one used for limits obtained with χ discussed in section 12. MC samples of QCD production modified by a contact interaction are created for values of Λ ranging from 4.0 TeV to 10.0 TeV. For the CI distributions, QCD K-factors are applied to the QCD-only components of the numerator and denominator of $F_\chi(m_{jj})$

JHEP01(2013)029

separately. This is done by subtracting the LO QCD cross section and adding the QCD cross section corrected for NLO effects.

Simulated $F_\chi(m_{jj})$ distributions are statistically smoothed by a fit in m_{jj}. For the pure QCD sample (corresponding to $\Lambda = \infty$), a second-order polynomial is used, while for the MC distributions with finite Λ, a Fermi function is added to the polynomial, which gives a good representation of the onset of contact interactions.

Next, all m_{jj} bins of the MC $F_\chi(m_{jj})$ distributions are interpolated in Λ using the same four-parameter interpolation function used for the χ analysis, creating a smooth predicted $F_\chi(m_{jj})$ surface as a function of m_{jj} and Λ. This surface enables integration in m_{jj} vs. Λ for continuous values of Λ.

Pseudo-experiments are then employed to construct a posterior probability, assuming a prior that is flat in $1/\Lambda^4$. This analysis sets a 95% CL lower limit on Λ at 7.6 TeV with an expected limit of 7.7 TeV.

15 Conclusions

Dijet mass and angular distributions have been measured by the ATLAS experiment over a large angular range and spanning dijet masses up to approximately 4.0 TeV, using 4.8 fb^{-1} of pp collision data at $\sqrt{s} = 7$ TeV. No resonance-like features have been observed in the dijet mass spectrum, and all angular distributions are consistent with QCD predictions. This analysis places limits on a variety of hypotheses for physics phenomena beyond the Standard Model, as summarised in table 4.

For $\sqrt{s} = 7$ TeV pp collisions at the LHC, the integrated luminosity used in the current studies represents a substantial increase over that available in previously published ATLAS dijet searches. Table 5 lists the previous and current expected limits from ATLAS studies using dijet analyses for three benchmark models: excited quarks, colour octet scalars, and contact interactions with destructive interference. The increase in the excited quark mass limit would have been greater by 0.10 TeV had there not been the long-standing problem with the default Pythia 6 q^* model, discussed in earlier sections.

For 2012 running, the collision energy of the LHC has been raised from 7 TeV to 8 TeV. The higher energy, and the associated rise in parton luminosity, will increase search sensitivities and the possibility of discoveries. The current 2011 analysis provides a reference for the study of energy-dependent effects once the 2012 data set has been analysed.

Acknowledgments

We thank Noriaki Kitazawa for the string resonance amplitude calculations and event samples.

We thank CERN for the very successful operation of the LHC, as well as the support staff from our institutions without whom ATLAS could not be operated efficiently.

We acknowledge the support of ANPCyT, Argentina; YerPhI, Armenia; ARC, Australia; BMWF and FWF, Austria; ANAS, Azerbaijan; SSTC, Belarus; CNPq and FAPESP, Brazil; NSERC, NRC and CFI, Canada; CERN; CONICYT, Chile; CAS, MOST and

JHEP01(2013)029

Model and Analysis Strategy	95% CL Limits [TeV]	
	Expected	Observed
Excited quark, mass of q^*		
Resonance in m_{jj}	2.94	2.83
Resonance in $F_\chi(m_{jj})$	2.85	2.75
Colour octet scalar, mass of s8		
Resonance in m_{jj}	1.97	1.86
Heavy W boson, mass of W'		
Resonance in m_{jj}	1.74	1.68
String resonances, scale of SR		
Resonance in m_{jj}	3.47	3.61
Quantum Black Hole for $n = 6$, M_D		
$F_\chi(m_{jj})$	4.16	4.03
χ, $m_{jj} > 2.6\,\text{TeV}$	4.20	4.11
Contact interaction, Λ, destructive interference		
$F_\chi(m_{jj})$	7.7	7.6
χ, $m_{jj} > 2.6\,\text{TeV}$	7.7	7.6

Table 4. The 95% CL lower limits on the masses and energy scales of the models examined in this study. All limit analyses are Bayesian, with statistical and systematic uncertainties included. For each NP hypothesis, the result corresponding to the highest expected limit is the result quoted in the abstract.

New Phenomenon	36 pb^{-1} [22]	1.0 fb^{-1} [23]	4.8 fb^{-1} current
Resonance in m_{jj}			
Excited quark, mass of q^*	2.07	2.81	2.94
Colour octet scalar, mass of s8	—	1.77	1.97
Angular distribution in χ			
Contact interaction, Λ	5.4	—	7.7

Table 5. ATLAS previous and current expected 95% CL upper limits [TeV] on new phenomena. The current expected limit for q^* cannot be compared directly to the two previous limits since they employed Pythia 6 samples with an error in the simulation of final state radiation. Had such samples been used in the current analysis, the expected q^* limit would be 0.10 TeV higher.

NSFC, China; COLCIENCIAS, Colombia; MSMT CR, MPO CR and VSC CR, Czech Republic; DNRF, DNSRC and Lundbeck Foundation, Denmark; EPLANET, ERC and NSRF, European Union; IN2P3-CNRS, CEA-DSM/IRFU, France; GNSF, Georgia; BMBF, DFG, HGF, MPG and AvH Foundation, Germany; GSRT and NSRF, Greece; ISF, MINERVA, GIF, DIP and Benoziyo Center, Israel; INFN, Italy; MEXT and JSPS, Japan; CNRST, Morocco; FOM and NWO, Netherlands; BRF and RCN, Norway; MNiSW, Poland; GRICES and FCT, Portugal; MERYS (MECTS), Romania; MES of Russia and ROSATOM, Rus-

JHEP01(2013)029

sian Federation; JINR; MSTD, Serbia; MSSR, Slovakia; ARRS and MVZT, Slovenia; DST/NRF, South Africa; MICINN, Spain; SRC and Wallenberg Foundation, Sweden; SER, SNSF and Cantons of Bern and Geneva, Switzerland; NSC, Taiwan; TAEK, Turkey; STFC, the Royal Society and Leverhulme Trust, United Kingdom; DOE and NSF, United States of America.

The crucial computing support from all WLCG partners is acknowledged gratefully, in particular from CERN and the ATLAS Tier-1 facilities at TRIUMF (Canada), NDGF (Denmark, Norway, Sweden), CC-IN2P3 (France), KIT/GridKA (Germany), INFN-CNAF (Italy), NL-T1 (Netherlands), PIC (Spain), ASGC (Taiwan), RAL (UK) and BNL (USA) and in the Tier-2 facilities worldwide.

A Limits on new resonant phenomena from the m_{jj} distribution

A.1 Excited quarks

m_{q^*} [GeV]	Observed	Expected	Expected $\pm1\sigma$	Expected $\pm2\sigma$	$\mathcal{A}$
1000	1.43	0.55	0.36/1.064	0.31/1.58	0.299
1200	0.30	0.36	0.27/0.66	0.23/0.99	0.403
1400	0.16	0.22	0.17/0.35	0.14/0.52	0.459
1600	0.16	0.15	0.12/0.25	0.098/0.37	0.481
1800	0.16	0.10	0.079/0.16	0.065/0.24	0.497
2000	0.12	0.071	0.054/0.11	0.043/0.16	0.501
2250	0.064	0.045	0.034/0.070	0.027/0.10	0.505
2500	0.050	0.032	0.023/0.050	0.018/0.071	0.511
2750	0.032	0.023	0.016/0.036	0.013/0.051	0.499
3000	0.017	0.016	0.012/0.024	0.0094/0.034	0.500
3250	0.0081	0.011	0.0086/0.017	0.0069/0.024	0.505
3500	0.0056	0.0081	0.0062/0.012	0.0049/0.016	0.499
3750	0.0041	0.0063	0.0047/0.0090	0.0037/0.013	0.493
4000	0.0034	0.0049	0.0036/0.0070	0.0028/0.010	0.484

Table 6. The 95% CL upper limit on $\sigma \times \mathcal{A}$ [pb] for excited quarks, q^*.

A.2 Colour octet scalars

m_{s8} [GeV]	Observed	Expected	Expected $\pm1\sigma$	Expected $\pm2\sigma$	$\mathcal{A}$
1300	0.40	0.68	0.38/1.45	0.31/2.20	0.339
1500	0.27	0.38	0.27/0.75	0.23/1.18	0.405
1700	0.24	0.27	0.20/0.52	0.17/0.79	0.443
2000	0.33	0.16	0.12/0.29	0.099/0.43	0.467
2500	0.17	0.084	0.059/0.14	0.049/0.21	0.484
3000	0.097	0.062	0.042/0.11	0.034/0.17	0.441
3500	0.034	0.049	0.036/0.079	0.030/0.12	0.390
4000	0.035	0.048	0.038/0.073	0.032/0.11	0.357

Table 7. The 95% CL upper limit on $\sigma \times \mathcal{A}$ [pb] for colour octets scalars, s8.

A.3 Heavy W boson

$m_{W'}$ [GeV]	Observed	Expected	Expected $\pm1\sigma$	Expected $\pm2\sigma$	$\mathcal{A}$
1100	0.65	0.46	0.32/0.88	0.27/1.30	0.286
1200	0.29	0.35	0.26/0.62	0.22/0.90	0.314
1400	0.15	0.21	0.16/0.33	0.13/0.48	0.345
1600	0.15	0.14	0.11/0.23	0.094/0.33	0.358
1800	0.13	0.099	0.077/0.16	0.063/0.23	0.353
2000	0.12	0.072	0.055/0.11	0.045/0.16	0.341
2400	0.065	0.042	0.031/0.064	0.025/0.090	0.293

Table 8. The 95% CL upper limit on $\sigma \times \mathcal{A} \times$ BR [pb] for Heavy W bosons, W'.

A.4 String resonances

m_{SR} [GeV]	Observed	Expected	Expected $\pm1\sigma$	Expected $\pm2\sigma$	$\mathcal{A}$
2000	0.094	0.059	0.041/0.080	0.032/0.12	0.449
2500	0.036	0.026	0.017/0.034	0.013/0.048	0.447
3000	0.012	0.012	0.0077/0.016	0.0061/0.022	0.452
3500	0.0041	0.0059	0.0036/0.0069	0.0028/0.010	0.464
4000	0.0021	0.0032	0.0020/0.0038	0.0016/0.0058	0.458
4500	0.0016	0.0023	0.0016/0.0029	0.0013/0.0040	0.478
5000	0.0013	0.0019	0.0012/0.0024	0.0010/0.0034	0.482

Table 9. The 95% CL upper limit on $\sigma \times \mathcal{A}$ [pb] for string resonances, SR.

References

[1] U. Baur, I. Hinchliffe and D. Zeppenfeld, *Excited quark production at hadron colliders*, *Int. J. Mod. Phys.* **A 2** (1987) 1285 [INSPIRE].

[2] U. Baur, M. Spira and P. Zerwas, *Excited quark and lepton production at hadron colliders*, *Phys. Rev.* **D 42** (1990) 815 [INSPIRE].

[3] P.H. Frampton and S.L. Glashow, *Chiral color: an alternative to the standard model*, *Phys. Lett.* **B 190** (1987) 157 [INSPIRE].

[4] P.H. Frampton and S.L. Glashow, *Unifiable chiral color with natural Glashow-Iliopoulos-Maiani mechanism*, *Phys. Rev. Lett.* **58** (1987) 2168 [INSPIRE].

[5] J. Bagger, C. Schmidt and S. King, *Axigluon production in hadronic collisions*, *Phys. Rev.* **D 37** (1988) 1188 [INSPIRE].

[6] T. Han, I. Lewis and Z. Liu, *Colored resonant signals at the LHC: largest rate and simplest topology*, *JHEP* **12** (2010) 085 [arXiv:1010.4309] [INSPIRE].

JHEP01(2013)029

[7] P. Meade and L. Randall, *Black holes and quantum gravity at the LHC*, *JHEP* **05** (2008) 003 [arXiv:0708.3017] [INSPIRE].

[8] L.A. Anchordoqui, J.L. Feng, H. Goldberg and A.D. Shapere, *Inelastic black hole production and large extra dimensions*, *Phys. Lett.* **B 594** (2004) 363 [hep-ph/0311365] [INSPIRE].

[9] S. Cullen, M. Perelstein and M.E. Peskin, *TeV strings and collider probes of large extra dimensions*, *Phys. Rev.* **D 62** (2000) 055012 [hep-ph/0001166] [INSPIRE].

[10] L.A. Anchordoqui, H. Goldberg, S. Nawata and T.R. Taylor, *Jet signals for low mass strings at the LHC*, *Phys. Rev. Lett.* **100** (2008) 171603 [arXiv:0712.0386] [INSPIRE].

[11] L.A. Anchordoqui et al., *LHC phenomenology for string hunters*, *Nucl. Phys.* **B 821** (2009) 181 [arXiv:0904.3547] [INSPIRE].

[12] N. Kitazawa, *A closer look at string resonances in dijet events at the LHC*, *JHEP* **10** (2010) 051 [arXiv:1008.4989] [INSPIRE].

[13] UA1 collaboration, G. Arnison et al., *Angular distributions and structure functions from two jet events at the CERN SPS $p\bar{p}$ collider*, *Phys. Lett.* **B 136** (1984) 294 [INSPIRE].

[14] UA2, BERN-CERN-COPENHAGEN-ORSAY-PAVIA-SACLAY collaboration, P. Bagnaia et al., *Measurement of jet production properties at the CERN $\bar{p}p$ collider*, *Phys. Lett.* **B 144** (1984) 283 [INSPIRE].

[15] CDF collaboration, T. Aaltonen et al., *Search for new particles decaying into dijets in proton-antiproton collisions at $\sqrt{s} = 1.96$ TeV*, *Phys. Rev.* **D 79** (2009) 112002 [arXiv:0812.4036] [INSPIRE].

[16] D0 collaboration, V. Abazov et al., *Measurement of dijet angular distributions at $\sqrt{s} = 1.96$ TeV and searches for quark compositeness and extra spatial dimensions*, *Phys. Rev. Lett.* **103** (2009) 191803 [arXiv:0906.4819] [INSPIRE].

[17] ATLAS collaboration, *Search for new particles in two-jet final states in 7 TeV proton-proton collisions with the ATLAS detector at the LHC*, *Phys. Rev. Lett.* **105** (2010) 161801 [arXiv:1008.2461] [INSPIRE].

[18] ATLAS collaboration, *Search for quark contact interactions in dijet angular distributions in pp collisions at $\sqrt{s} = 7$ TeV measured with the ATLAS detector*, *Phys. Lett.* **B 694** (2011) 327 [arXiv:1009.5069] [INSPIRE].

[19] CMS collaboration, *Search for resonances in the dijet mass spectrum from 7 TeV pp collisions at CMS*, *Phys. Lett.* **B 704** (2011) 123 [arXiv:1107.4771] [INSPIRE].

[20] CMS collaboration, *Search for quark compositeness with the dijet centrality ratio in pp collisions at $\sqrt{s} = 7$ TeV*, *Phys. Rev. Lett.* **105** (2010) 262001 [arXiv:1010.4439] [INSPIRE].

[21] CMS collaboration, *Measurement of dijet angular distributions and search for quark compositeness in pp collisions at $\sqrt{s} = 7$ TeV*, *Phys. Rev. Lett.* **106** (2011) 201804 [arXiv:1102.2020] [INSPIRE].

[22] ATLAS collaboration, *Search for new physics in dijet mass and angular distributions in pp collisions at $\sqrt{s} = 7$ TeV measured with the ATLAS detector*, *New J. Phys.* **13** (2011) 053044 [arXiv:1103.3864] [INSPIRE].

[23] ATLAS collaboration, G. Aad et al., *Search for new physics in the dijet mass distribution using 1 fb^{-1} of pp collision data at $\sqrt{s} = 7$ TeV collected by the ATLAS detector*, *Phys. Lett.* **B 708** (2012) 37 [arXiv:1108.6311] [INSPIRE].

JHEP01(2013)029

[24] ATLAS collaboration, *Luminosity determination in pp collisions at $\sqrt{s} = 7$ TeV using the ATLAS detector in 2011*, ATLAS-CONF-2011-116 (2011).

[25] ATLAS collaboration, *Luminosity determination in pp collisions at $\sqrt{s} = 7$ TeV using the ATLAS detector at the LHC*, *Eur. Phys. J.* **C 71** (2011) 1630 [arXiv:1101.2185] [INSPIRE].

[26] ATLAS collaboration, *The ATLAS experiment at the CERN Large Hadron Collider*, 2008 *JINST* **3** S08003 [INSPIRE].

[27] W. Lampl et al., *Calorimeter clustering algorithms: description and performance*, ATL-LARG-PUB-2008-002 (2008).

[28] M. Cacciari, G.P. Salam and G. Soyez, *The anti-k_t jet clustering algorithm*, *JHEP* **04** (2008) 063 [arXiv:0802.1189] [INSPIRE].

[29] M. Cacciari and G.P. Salam, *Dispelling the N^3 myth for the k_t jet-finder*, *Phys. Lett.* **B 641** (2006) 57 [hep-ph/0512210] [INSPIRE].

[30] ATLAS collaboration, *Jet energy scale and its systematic uncertainty in proton-proton collisions at $\sqrt{s} = 7$ TeV with ATLAS 2011 data*, ATLAS-CONF-2011-032 (2011).

[31] ATLAS collaboration, *Jet energy measurement with the ATLAS detector in proton-proton collisions at $\sqrt{s} = 7$ TeV*, arXiv:1112.6426 [INSPIRE].

[32] ATLAS collaboration, *In situ jet pseudorapidity intercalibration of the ATLAS detector using dijet events in $\sqrt{s} = 7$ TeV proton-proton 2011 data*, ATLAS-CONF-2012-124 (2012).

[33] ATLAS collaboration, *Jet energy resolution in proton-proton collisions at $\sqrt{s} = 7$ TeV recorded in 2010 with the ATLAS detector*, arXiv:1210.6210 [CERN-PH-EP-2012-191].

[34] ATLAS collaboration, *Selection of jets produced in proton-proton collisions with the ATLAS detector using 2011 data*, ATLAS-CONF-2012-020 (2012).

[35] G. Choudalakis and D. Casadei, *Plotting the differences between data and expectation*, *Eur. Phys. J. Plus* **127** (2012) 25 [arXiv:1111.2062].

[36] CDF collaboration, *Global search for new physics with 2.0 fb^{-1} at CDF*, *Phys. Rev.* **D 79** (2009) 011101 [arXiv:0809.3781] [INSPIRE].

[37] G. Choudalakis, *On hypothesis testing, trials factor, hypertests and the BumpHunter*, arXiv:1101.0390 [INSPIRE].

[38] L. Lyons, *Open statistical issues in particle physics*, *Ann. Appl. Stat.* **2** (2008) 887 [INSPIRE].

[39] T. Sjöstrand, S. Mrenna and P.Z. Skands, *PYTHIA 6.4 physics and manual*, *JHEP* **05** (2006) 026 [hep-ph/0603175] [INSPIRE].

[40] ATALS collaboration, *ATLAS tunes of PYTHIA 6 and Pythia 8 for MC11*, ATL-PHYS-PUB-2011-009 (2011).

[41] A. Sherstnev and R. Thorne, *Parton distributions for LO generators*, *Eur. Phys. J.* **C 55** (2008) 553 [arXiv:0711.2473] [INSPIRE].

[42] E. Richter-Was et al., *ATLFAST 2.0, a fast simulation package for ATLAS*, ATL-PHYS-98-131 (1998).

[43] ATLAS collaboration, *The simulation principle and performance of the ATLAS fast calorimeter simulation FastCaloSim*, ATL-PHYS-PUB-2010-013 (2010).

[44] ATLAS collaboration, *The ATLAS simulation infrastructure*, *Eur. Phys. J.* **C 70** (2010) 823 [arXiv:1005.4568] [INSPIRE].

JHEP01(2013)029

[45] GEANT4 collaboration, S. Agostinelli et al., *GEANT4: a simulation toolkit*, *Nucl. Instrum. Meth.* **A 506** (2003) 250 [INSPIRE].

[46] T. Sjöstrand, S. Mrenna and P.Z. Skands, *A brief introduction to PYTHIA 8.1*, *Comput. Phys. Commun.* **178** (2008) 852 [arXiv:0710.3820] [INSPIRE].

[47] Z. Nagy, *Three jet cross-sections in hadron hadron collisions at next-to-leading order*, *Phys. Rev. Lett.* **88** (2002) 122003 [hep-ph/0110315] [INSPIRE].

[48] Z. Nagy, *Next-to-leading order calculation of three jet observables in hadron hadron collision*, *Phys. Rev.* **D 68** (2003) 094002 [hep-ph/0307268] [INSPIRE].

[49] S. Catani and M. Seymour, *A general algorithm for calculating jet cross-sections in NLO QCD*, *Nucl. Phys.* **B 485** (1997) 291 [*Erratum ibid.* **B 510** (1998) 503-504] [hep-ph/9605323] [INSPIRE].

[50] H.-L. Lai et al., *New parton distributions for collider physics*, *Phys. Rev.* **D 82** (2010) 074024 [arXiv:1007.2241] [INSPIRE].

[51] S. Moretti, M. Nolten and D. Ross, *Weak corrections to four-parton processes*, *Nucl. Phys.* **B 759** (2006) 50 [hep-ph/0606201] [INSPIRE].

[52] J.M. Campbell, J.W. Huston and W.J. Stirling, *Hard interactions of quarks and gluons: a primer for LHC physics*, *Rept. Prog. Phys.* **70** (2007) 89 [hep-ph/0611148] [INSPIRE].

[53] E. Eichten, I. Hinchliffe, K.D. Lane and C. Quigg, *Super collider physics*, *Rev. Mod. Phys.* **56** (1984) 579 [*Addendum ibid.* **58** (1986) 1065] [INSPIRE].

[54] P. Chiappetta and M. Perrottet, *Possible bounds on compositeness from inclusive one jet production in large hadron colliders*, *Phys. Lett.* **B 253** (1991) 489 [INSPIRE].

[55] G. Altarelli, B. Mele and M. Ruiz-Altaba, *Searching for new heavy vector bosons in $p\bar{p}$ colliders*, *Z. Phys.* **C 45** (1989) 109 [*Erratum ibid.* **C 47** (1990) 676] [INSPIRE].

[56] CMS collaboration, S. Chatrchyan et al., *Search for a W' boson decaying to a muon and a neutrino in pp collisions at $\sqrt{s} = 7$ TeV*, *Phys. Lett.* **B 701** (2011) 160 [arXiv:1103.0030] [INSPIRE].

[57] ATLAS collaboration, G. Aad et al., *Search for a heavy gauge boson decaying to a charged lepton and a neutrino in 1 fb^{-1} of pp collisions at $\sqrt{s} = 7$ TeV using the ATLAS detector*, *Phys. Lett.* **B 705** (2011) 28 [arXiv:1108.1316] [INSPIRE].

[58] J. Alwall, M. Herquet, F. Maltoni, O. Mattelaer and T. Stelzer, *MadGraph 5: going beyond*, *JHEP* **06** (2011) 128 [arXiv:1106.0522] [INSPIRE].

[59] J. Pumplin et al., *New generation of parton distributions with uncertainties from global QCD analysis*, *JHEP* **07** (2002) 012 [hep-ph/0201195] [INSPIRE].

[60] D.-C. Dai et al., *BlackMax: a black-hole event generator with rotation, recoil, split branes and brane tension*, *Phys. Rev.* **D 77** (2008) 076007 [arXiv:0711.3012] [INSPIRE].

[61] R. Hamberg, W. van Neerven and T. Matsuura, *A complete calculation of the order α_s^2 correction to the Drell-Yan K factor*, *Nucl. Phys.* **B 359** (1991) 343 [*Erratum ibid.* **B 644** (2002) 403-404] [INSPIRE].

[62] C. Carloni Calame, G. Montagna, O. Nicrosini and A. Vicini, *Precision electroweak calculation of the charged current Drell-Yan process*, *JHEP* **12** (2006) 016 [hep-ph/0609170] [INSPIRE].

JHEP01(2013)029

[63] C. Carloni Calame, G. Montagna, O. Nicrosini and A. Vicini, *Precision electroweak calculation of the production of a high transverse-momentum lepton pair at hadron colliders*, *JHEP* **10** (2007) 109 [arXiv:0710.1722] [INSPIRE].

[64] A. Martin, W. Stirling, R. Thorne and G. Watt, *Parton distributions for the LHC*, *Eur. Phys. J.* **C 63** (2009) 189 [arXiv:0901.0002] [INSPIRE].

[65] A. Pukhov, *CalcHEP 2.3: MSSM, structure functions, event generation, batchs and generation of matrix elements for other packages*, hep-ph/0412191 [INSPIRE].

[66] H. Georgi, E.E. Jenkins and E.H. Simmons, *The ununified standard model*, *Nucl. Phys.* **B 331** (1990) 541 [INSPIRE].

[67] C. Grojean, E. Salvioni and R. Torre, *A weakly constrained W' at the early LHC*, *JHEP* **07** (2011) 002 [arXiv:1103.2761] [INSPIRE].

[68] M. Cvetič and J.C. Pati, $N = 1$ *supergravity within the minimal left-right symmetric model*, *Phys. Lett.* **B 135** (1984) 57 [INSPIRE].

[69] Y. Mimura and S. Nandi, *Orbifold breaking of left-right gauge symmetry*, *Phys. Lett.* **B 538** (2002) 406 [hep-ph/0203126] [INSPIRE].

JHEP01(2013)029

The ATLAS collaboration

G. Aad[48], T. Abajyan[21], B. Abbott[111], J. Abdallah[12], S. Abdel Khalek[115], A.A. Abdelalim[49], O. Abdinov[11], R. Aben[105], B. Abi[112], M. Abolins[88], O.S. AbouZeid[158], H. Abramowicz[153], H. Abreu[136], B.S. Acharya[164a,164b], L. Adamczyk[38], D.L. Adams[25], T.N. Addy[56], J. Adelman[176], S. Adomeit[98], P. Adragna[75], T. Adye[129], S. Aefsky[23], J.A. Aguilar-Saavedra[124b,a], M. Agustoni[17], M. Aharrouche[81], S.P. Ahlen[22], F. Ahles[48], A. Ahmad[148], M. Ahsan[41], G. Aielli[133a,133b], T.P.A. Åkesson[79], G. Akimoto[155], A.V. Akimov[94], M.S. Alam[2], M.A. Alam[76], J. Albert[169], S. Albrand[55], M. Aleksa[30], I.N. Aleksandrov[64], F. Alessandria[89a], C. Alexa[26a], G. Alexander[153], G. Alexandre[49], T. Alexopoulos[10], M. Alhroob[164a,164c], M. Aliev[16], G. Alimonti[89a], J. Alison[120], B.M.M. Allbrooke[18], P.P. Allport[73], S.E. Allwood-Spiers[53], J. Almond[82], A. Aloisio[102a,102b], R. Alon[172], A. Alonso[79], F. Alonso[70], A. Altheimer[35], B. Alvarez Gonzalez[88], M.G. Alviggi[102a,102b], K. Amako[65], C. Amelung[23], V.V. Ammosov[128,*], S.P. Amor Dos Santos[124a], A. Amorim[124a,b], N. Amram[153], C. Anastopoulos[30], L.S. Ancu[17], N. Andari[115], T. Andeen[35], C.F. Anders[58b], G. Anders[58a], K.J. Anderson[31], A. Andreazza[89a,89b], V. Andrei[58a], M-L. Andrieux[55], X.S. Anduaga[70], S. Angelidakis[9], P. Anger[44], A. Angerami[35], F. Anghinolfi[30], A. Anisenkov[107], N. Anjos[124a], A. Annovi[47], A. Antonaki[9], M. Antonelli[47], A. Antonov[96], J. Antos[144b], F. Anulli[132a], M. Aoki[101], S. Aoun[83], L. Aperio Bella[5], R. Apolle[118,c], G. Arabidze[88], I. Aracena[143], Y. Arai[65], A.T.H. Arce[45], S. Arfaoui[148], J-F. Arguin[93], S. Argyropoulos[42], E. Arik[19a,*], M. Arik[19a], A.J. Armbruster[87], O. Arnaez[81], V. Arnal[80], C. Arnault[115], A. Artamonov[95], G. Artoni[132a,132b], D. Arutinov[21], S. Asai[155], S. Ask[28], B. Åsman[146a,146b], L. Asquith[6], K. Assamagan[25], A. Astbury[169], M. Atkinson[165], B. Aubert[5], E. Auge[115], K. Augsten[127], M. Aurousseau[145a], G. Avolio[30], R. Avramidou[10], D. Axen[168], G. Azuelos[93,d], Y. Azuma[155], M.A. Baak[30], G. Baccaglioni[89a], C. Bacci[134a,134b], A.M. Bach[15], H. Bachacou[136], K. Bachas[30], M. Backes[49], M. Backhaus[21], J. Backus Mayes[143], E. Badescu[26a], P. Bagnaia[132a,132b], S. Bahinipati[3], Y. Bai[33a], D.C. Bailey[158], T. Bain[158], J.T. Baines[129], O.K. Baker[176], M.D. Baker[25], S. Baker[77], P. Balek[126], E. Banas[39], P. Banerjee[93], Sw. Banerjee[173], D. Banfi[30], A. Bangert[150], V. Bansal[169], H.S. Bansil[18], L. Barak[172], S.P. Baranov[94], A. Barbaro Galtieri[15], T. Barber[48], E.L. Barberio[86], D. Barberis[50a,50b], M. Barbero[21], D.Y. Bardin[64], T. Barillari[99], M. Barisonzi[175], T. Barklow[143], N. Barlow[28], B.M. Barnett[129], R.M. Barnett[15], A. Baroncelli[134a], G. Barone[49], A.J. Barr[118], F. Barreiro[80], J. Barreiro Guimarães da Costa[57], P. Barrillon[115], R. Bartoldus[143], A.E. Barton[71], V. Bartsch[149], A. Basye[165], R.L. Bates[53], L. Batkova[144a], J.R. Batley[28], A. Battaglia[17], M. Battistin[30], F. Bauer[136], H.S. Bawa[143,e], S. Beale[98], T. Beau[78], P.H. Beauchemin[161], R. Beccherle[50a], P. Bechtle[21], H.P. Beck[17], A.K. Becker[175], S. Becker[98], M. Beckingham[138], K.H. Becks[175], A.J. Beddall[19c], A. Beddall[19c], S. Bedikian[176], V.A. Bednyakov[64], C.P. Bee[83], L.J. Beemster[105], M. Begel[25], S. Behar Harpaz[152], P.K. Behera[62], M. Beimforde[99], C. Belanger-Champagne[85], P.J. Bell[49], W.H. Bell[49], G. Bella[153], L. Bellagamba[20a], M. Bellomo[30], A. Belloni[57], O. Beloborodova[107,f], K. Belotskiy[96], O. Beltramello[30], O. Benary[153], D. Benchekroun[135a], K. Bendtz[146a,146b], N. Benekos[165], Y. Benhammou[153], E. Benhar Noccioli[49], J.A. Benitez Garcia[159b], D.P. Benjamin[45], M. Benoit[115], J.R. Bensinger[23], K. Benslama[130], S. Bentvelsen[105], D. Berge[30], E. Bergeaas Kuutmann[42], N. Berger[5], F. Berghaus[169], E. Berglund[105], J. Beringer[15], P. Bernat[77], R. Bernhard[48], C. Bernius[25], T. Berry[76], C. Bertella[83], A. Bertin[20a,20b], F. Bertolucci[122a,122b], M.I. Besana[89a,89b], G.J. Besjes[104], N. Besson[136], S. Bethke[99], W. Bhimji[46], R.M. Bianchi[30], L. Bianchini[23], M. Bianco[72a,72b], O. Biebel[98], S.P. Bieniek[77], K. Bierwagen[54], J. Biesiada[15], M. Biglietti[134a], H. Bilokon[47], M. Bindi[20a,20b], S. Binet[115], A. Bingul[19c], C. Bini[132a,132b], C. Biscarat[178], B. Bittner[99], K.M. Black[22], R.E. Blair[6], J.-B. Blanchard[136], G. Blanchot[30], T. Blazek[144a], I. Bloch[42],

JHEP01(2013)029

C. Blocker[23], J. Blocki[39], A. Blondel[49], W. Blum[81], U. Blumenschein[54], G.J. Bobbink[105], V.B. Bobrovnikov[107], S.S. Bocchetta[79], A. Bocci[45], C.R. Boddy[118], M. Boehler[48], J. Boek[175], N. Boelaert[36], J.A. Bogaerts[30], A. Bogdanchikov[107], A. Bogouch[90,*], C. Bohm[146a], J. Bohm[125], V. Boisvert[76], T. Bold[38], V. Boldea[26a], N.M. Bolnet[136], M. Bomben[78], M. Bona[75], M. Boonekamp[136], S. Bordoni[78], C. Borer[17], A. Borisov[128], G. Borissov[71], I. Borjanovic[13a], M. Borri[82], S. Borroni[87], J. Bortfeldt[98], V. Bortolotto[134a,134b], K. Bos[105], D. Boscherini[20a], M. Bosman[12], H. Boterenbrood[105], J. Bouchami[93], J. Boudreau[123], E.V. Bouhova-Thacker[71], D. Boumediene[34], C. Bourdarios[115], N. Bousson[83], A. Boveia[31], J. Boyd[30], I.R. Boyko[64], I. Bozovic-Jelisavcic[13b], J. Bracinik[18], P. Branchini[134a], A. Brandt[8], G. Brandt[118], O. Brandt[54], U. Bratzler[156], B. Brau[84], J.E. Brau[114], H.M. Braun[175,*], S.F. Brazzale[164a,164c], B. Brelier[158], J. Bremer[30], K. Brendlinger[120], R. Brenner[166], S. Bressler[172], D. Britton[53], F.M. Brochu[28], I. Brock[21], R. Brock[88], F. Broggi[89a], C. Bromberg[88], J. Bronner[99], G. Brooijmans[35], T. Brooks[76], W.K. Brooks[32b], G. Brown[82], H. Brown[8], P.A. Bruckman de Renstrom[39], D. Bruncko[144b], R. Bruneliere[48], S. Brunet[60], A. Bruni[20a], G. Bruni[20a], M. Bruschi[20a], T. Buanes[14], Q. Buat[55], F. Bucci[49], J. Buchanan[118], P. Buchholz[141], R.M. Buckingham[118], A.G. Buckley[46], S.I. Buda[26a], I.A. Budagov[64], B. Budick[108], V. Büscher[81], L. Bugge[117], O. Bulekov[96], A.C. Bundock[73], M. Bunse[43], T. Buran[117], H. Burckhart[30], S. Burdin[73], T. Burgess[14], S. Burke[129], E. Busato[34], P. Bussey[53], C.P. Buszello[166], B. Butler[143], J.M. Butler[22], C.M. Buttar[53], J.M. Butterworth[77], W. Buttinger[28], M. Byszewski[30], S. Cabrera Urbán[167], D. Caforio[20a,20b], O. Cakir[4a], P. Calafiura[15], G. Calderini[78], P. Calfayan[98], R. Calkins[106], L.P. Caloba[24a], R. Caloi[132a,132b], D. Calvet[34], S. Calvet[34], R. Camacho Toro[34], P. Camarri[133a,133b], D. Cameron[117], L.M. Caminada[15], R. Caminal Armadans[12], S. Campana[30], M. Campanelli[77], V. Canale[102a,102b], F. Canelli[31], A. Canepa[159a], J. Cantero[80], R. Cantrill[76], L. Capasso[102a,102b], M.D.M. Capeans Garrido[30], I. Caprini[26a], M. Caprini[26a], D. Capriotti[99], M. Capua[37a,37b], R. Caputo[81], R. Cardarelli[133a], T. Carli[30], G. Carlino[102a], L. Carminati[89a,89b], B. Caron[85], S. Caron[104], E. Carquin[32b], G.D. Carrillo-Montoya[145b], A.A. Carter[75], J.R. Carter[28], J. Carvalho[124a,g], D. Casadei[108], M.P. Casado[12], M. Cascella[122a,122b], C. Caso[50a,50b,*], A.M. Castaneda Hernandez[173,h], E. Castaneda-Miranda[173], V. Castillo Gimenez[167], N.F. Castro[124a], G. Cataldi[72a], P. Catastini[57], A. Catinaccio[30], J.R. Catmore[30], A. Cattai[30], G. Cattani[133a,133b], S. Caughron[88], V. Cavaliere[165], P. Cavalleri[78], D. Cavalli[89a], M. Cavalli-Sforza[12], V. Cavasinni[122a,122b], F. Ceradini[134a,134b], A.S. Cerqueira[24b], A. Cerri[30], L. Cerrito[75], F. Cerutti[47], S.A. Cetin[19b], A. Chafaq[135a], D. Chakraborty[106], I. Chalupkova[126], K. Chan[3], P. Chang[165], B. Chapleau[85], J.D. Chapman[28], J.W. Chapman[87], E. Chareyre[78], D.G. Charlton[18], V. Chavda[82], C.A. Chavez Barajas[30], S. Cheatham[85], S. Chekanov[6], S.V. Chekulaev[159a], G.A. Chelkov[64], M.A. Chelstowska[104], C. Chen[63], H. Chen[25], S. Chen[33c], X. Chen[173], Y. Chen[35], Y. Cheng[31], A. Cheplakov[64], R. Cherkaoui El Moursli[135e], V. Chernyatin[25], E. Cheu[7], S.L. Cheung[158], L. Chevalier[136], G. Chiefari[102a,102b], L. Chikovani[51a,*], J.T. Childers[30], A. Chilingarov[71], G. Chiodini[72a], A.S. Chisholm[18], R.T. Chislett[77], A. Chitan[26a], M.V. Chizhov[64], G. Choudalakis[31], S. Chouridou[137], I.A. Christidi[77], A. Christov[48], D. Chromek-Burckhart[30], M.L. Chu[151], J. Chudoba[125], G. Ciapetti[132a,132b], A.K. Ciftci[4a], R. Ciftci[4a], D. Cinca[34], V. Cindro[74], C. Ciocca[20a,20b], A. Ciocio[15], M. Cirilli[87], P. Cirkovic[13b], Z.H. Citron[172], M. Citterio[89a], M. Ciubancan[26a], A. Clark[49], P.J. Clark[46], R.N. Clarke[15], W. Cleland[123], J.C. Clemens[83], B. Clement[55], C. Clement[146a,146b], Y. Coadou[83], M. Cobal[164a,164c], A. Coccaro[138], J. Cochran[63], L. Coffey[23], J.G. Cogan[143], J. Coggeshall[165], E. Cogneras[178], J. Colas[5], S. Cole[106], A.P. Colijn[105], N.J. Collins[18], C. Collins-Tooth[53], J. Collot[55], T. Colombo[119a,119b], G. Colon[84], G. Compostella[99], P. Conde Muiño[124a], E. Coniavitis[166], M.C. Conidi[12], S.M. Consonni[89a,89b], V. Consorti[48], S. Constantinescu[26a], C. Conta[119a,119b], G. Conti[57], F. Conventi[102a,i], M. Cooke[15], B.D. Cooper[77],

JHEP01(2013)029

A.M. Cooper-Sarkar[118], K. Copic[15], T. Cornelissen[175], M. Corradi[20a], F. Corriveau[85,j], A. Cortes-Gonzalez[165], G. Cortiana[99], G. Costa[89a], M.J. Costa[167], D. Costanzo[139], D. Côté[30], L. Courneyea[169], G. Cowan[76], C. Cowden[28], B.E. Cox[82], K. Cranmer[108], F. Crescioli[122a,122b], M. Cristinziani[21], G. Crosetti[37a,37b], S. Crépé-Renaudin[55], C.-M. Cuciuc[26a], C. Cuenca Almenar[176], T. Cuhadar Donszelmann[139], J. Cummings[176], M. Curatolo[47], C.J. Curtis[18], C. Cuthbert[150], P. Cwetanski[60], H. Czirr[141], P. Czodrowski[44], Z. Czyczula[176], S. D'Auria[53], M. D'Onofrio[73], A. D'Orazio[132a,132b], M.J. Da Cunha Sargedas De Sousa[124a], C. Da Via[82], W. Dabrowski[38], A. Dafinca[118], T. Dai[87], C. Dallapiccola[84], M. Dam[36], M. Dameri[50a,50b], D.S. Damiani[137], H.O. Danielsson[30], V. Dao[49], G. Darbo[50a], G.L. Darlea[26b], J.A. Dassoulas[42], W. Davey[21], T. Davidek[126], N. Davidson[86], R. Davidson[71], E. Davies[118,c], M. Davies[93], O. Davignon[78], A.R. Davison[77], Y. Davygora[58a], E. Dawe[142], I. Dawson[139], R.K. Daya-Ishmukhametova[23], K. De[8], R. de Asmundis[102a], S. De Castro[20a,20b], S. De Cecco[78], J. de Graat[98], N. De Groot[104], P. de Jong[105], C. De La Taille[115], H. De la Torre[80], F. De Lorenzi[63], L. de Mora[71], L. De Nooij[105], D. De Pedis[132a], A. De Salvo[132a], U. De Sanctis[164a,164c], A. De Santo[149], J.B. De Vivie De Regie[115], G. De Zorzi[132a,132b], W.J. Dearnaley[71], R. Debbe[25], C. Debenedetti[46], B. Dechenaux[55], D.V. Dedovich[64], J. Degenhardt[120], J. Del Peso[80], T. Del Prete[122a,122b], T. Delemontex[55], M. Deliyergiyev[74], A. Dell'Acqua[30], L. Dell'Asta[22], M. Della Pietra[102a,i], D. della Volpe[102a,102b], M. Delmastro[5], P.A. Delsart[55], C. Deluca[105], S. Demers[176], M. Demichev[64], B. Demirkoz[12,k], S.P. Denisov[128], D. Derendarz[39], J.E. Derkaoui[135d], F. Derue[78], P. Dervan[73], K. Desch[21], E. Devetak[148], P.O. Deviveiros[105], A. Dewhurst[129], B. DeWilde[148], S. Dhaliwal[158], R. Dhullipudi[25,l], A. Di Ciaccio[133a,133b], L. Di Ciaccio[5], C. Di Donato[102a,102b], A. Di Girolamo[30], B. Di Girolamo[30], S. Di Luise[134a,134b], A. Di Mattia[173], B. Di Micco[30], R. Di Nardo[47], A. Di Simone[133a,133b], R. Di Sipio[20a,20b], M.A. Diaz[32a], E.B. Diehl[87], J. Dietrich[42], T.A. Dietzsch[58a], S. Diglio[86], K. Dindar Yagci[40], J. Dingfelder[21], F. Dinut[26a], C. Dionisi[132a,132b], P. Dita[26a], S. Dita[26a], F. Dittus[30], F. Djama[83], T. Djobava[51b], M.A.B. do Vale[24c], A. Do Valle Wemans[124a,m], T.K.O. Doan[5], M. Dobbs[85], D. Dobos[30], E. Dobson[30,n], J. Dodd[35], C. Doglioni[49], T. Doherty[53], Y. Doi[65,*], J. Dolejsi[126], I. Dolenc[74], Z. Dolezal[126], B.A. Dolgoshein[96,*], T. Dohmae[155], M. Donadelli[24d], J. Donini[34], J. Dopke[30], A. Doria[102a], A. Dos Anjos[173], A. Dotti[122a,122b], M.T. Dova[70], A.D. Doxiadis[105], A.T. Doyle[53], N. Dressnandt[120], M. Dris[10], J. Dubbert[99], S. Dube[15], E. Duchovni[172], G. Duckeck[98], D. Duda[175], A. Dudarev[30], F. Dudziak[63], M. Dührssen[30], I.P. Duerdoth[82], L. Duflot[115], M-A. Dufour[85], L. Duguid[76], M. Dunford[58a], H. Duran Yildiz[4a], R. Duxfield[139], M. Dwuznik[38], M. Düren[52], W.L. Ebenstein[45], J. Ebke[98], S. Eckweiler[81], K. Edmonds[81], W. Edson[2], C.A. Edwards[76], N.C. Edwards[53], W. Ehrenfeld[42], T. Eifert[143], G. Eigen[14], K. Einsweiler[15], E. Eisenhandler[75], T. Ekelof[166], M. El Kacimi[135c], M. Ellert[166], S. Elles[5], F. Ellinghaus[81], K. Ellis[75], N. Ellis[30], J. Elmsheuser[98], M. Elsing[30], D. Emeliyanov[129], R. Engelmann[148], A. Engl[98], B. Epp[61], J. Erdmann[54], A. Ereditato[17], D. Eriksson[146a], J. Ernst[2], M. Ernst[25], J. Ernwein[136], D. Errede[165], S. Errede[165], E. Ertel[81], M. Escalier[115], H. Esch[43], C. Escobar[123], X. Espinal Curull[12], B. Esposito[47], F. Etienne[83], A.I. Etienvre[136], E. Etzion[153], D. Evangelakou[54], H. Evans[60], L. Fabbri[20a,20b], C. Fabre[30], R.M. Fakhrutdinov[128], S. Falciano[132a], Y. Fang[173], M. Fanti[89a,89b], A. Farbin[8], A. Farilla[134a], J. Farley[148], T. Farooque[158], S. Farrell[163], S.M. Farrington[170], P. Farthouat[30], F. Fassi[167], P. Fassnacht[30], D. Fassouliotis[9], B. Fatholahzadeh[158], A. Favareto[89a,89b], L. Fayard[115], S. Fazio[37a,37b], R. Febbraro[34], P. Federic[144a], O.L. Fedin[121], W. Fedorko[88], M. Fehling-Kaschek[48], L. Feligioni[83], C. Feng[33d], E.J. Feng[6], A.B. Fenyuk[128], J. Ferencei[144b], W. Fernando[6], S. Ferrag[53], J. Ferrando[53], V. Ferrara[42], A. Ferrari[166], P. Ferrari[105], R. Ferrari[119a], D.E. Ferreira de Lima[53], A. Ferrer[167], D. Ferrere[49], C. Ferretti[87], A. Ferretto Parodi[50a,50b], M. Fiascaris[31], F. Fiedler[81], A. Filipčič[74], F. Filthaut[104],

JHEP01(2013)029

M. Fincke-Keeler[169], M.C.N. Fiolhais[124a,g], L. Fiorini[167], A. Firan[40], G. Fischer[42], M.J. Fisher[109], M. Flechl[48], I. Fleck[141], J. Fleckner[81], P. Fleischmann[174], S. Fleischmann[175], T. Flick[175], A. Floderus[79], L.R. Flores Castillo[173], M.J. Flowerdew[99], T. Fonseca Martin[17], A. Formica[136], A. Forti[82], D. Fortin[159a], D. Fournier[115], A.J. Fowler[45], H. Fox[71], P. Francavilla[12], M. Franchini[20a,20b], S. Franchino[119a,119b], D. Francis[30], T. Frank[172], M. Franklin[57], S. Franz[30], M. Fraternali[119a,119b], S. Fratina[120], S.T. French[28], C. Friedrich[42], F. Friedrich[44], R. Froeschl[30], D. Froidevaux[30], J.A. Frost[28], C. Fukunaga[156], E. Fullana Torregrosa[30], B.G. Fulsom[143], J. Fuster[167], C. Gabaldon[30], O. Gabizon[172], T. Gadfort[25], S. Gadomski[49], G. Gagliardi[50a,50b], P. Gagnon[60], C. Galea[98], B. Galhardo[124a], E.J. Gallas[118], V. Gallo[17], B.J. Gallop[129], P. Gallus[125], K.K. Gan[109], Y.S. Gao[143,e], A. Gaponenko[15], F. Garberson[176], M. Garcia-Sciveres[15], C. García[167], J.E. García Navarro[167], R.W. Gardner[31], N. Garelli[30], H. Garitaonandia[105], V. Garonne[30], C. Gatti[47], G. Gaudio[119a], B. Gaur[141], L. Gauthier[136], P. Gauzzi[132a,132b], I.L. Gavrilenko[94], C. Gay[168], G. Gaycken[21], E.N. Gazis[10], P. Ge[33d], Z. Gecse[168], C.N.P. Gee[129], D.A.A. Geerts[105], Ch. Geich-Gimbel[21], K. Gellerstedt[146a,146b], C. Gemme[50a], A. Gemmell[53], M.H. Genest[55], S. Gentile[132a,132b], M. George[54], S. George[76], P. Gerlach[175], A. Gershon[153], C. Geweniger[58a], H. Ghazlane[135b], N. Ghodbane[34], B. Giacobbe[20a], S. Giagu[132a,132b], V. Giakoumopoulou[9], V. Giangiobbe[12], F. Gianotti[30], B. Gibbard[25], A. Gibson[158], S.M. Gibson[30], M. Gilchriese[15], D. Gillberg[29], A.R. Gillman[129], D.M. Gingrich[3,d], J. Ginzburg[153], N. Giokaris[9], M.P. Giordani[164c], R. Giordano[102a,102b], F.M. Giorgi[16], P. Giovannini[99], P.F. Giraud[136], D. Giugni[89a], M. Giunta[93], B.K. Gjelsten[117], L.K. Gladilin[97], C. Glasman[80], J. Glatzer[21], A. Glazov[42], K.W. Glitza[175], G.L. Glonti[64], J.R. Goddard[75], J. Godfrey[142], J. Godlewski[30], M. Goebel[42], T. Göpfert[44], C. Goeringer[81], C. Gössling[43], S. Goldfarb[87], T. Golling[176], A. Gomes[124a,b], L.S. Gomez Fajardo[42], R. Gonçalo[76], J. Goncalves Pinto Firmino Da Costa[42], L. Gonella[21], S. González de la Hoz[167], G. Gonzalez Parra[12], M.L. Gonzalez Silva[27], S. Gonzalez-Sevilla[49], J.J. Goodson[148], L. Goossens[30], P.A. Gorbounov[95], H.A. Gordon[25], I. Gorelov[103], G. Gorfine[175], B. Gorini[30], E. Gorini[72a,72b], A. Gorišek[74], E. Gornicki[39], A.T. Goshaw[6], M. Gosselink[105], M.I. Gostkin[64], I. Gough Eschrich[163], M. Gouighri[135a], D. Goujdami[135c], M.P. Goulette[49], A.G. Goussiou[138], C. Goy[5], S. Gozpinar[23], I. Grabowska-Bold[38], P. Grafström[20a,20b], K-J. Grahn[42], E. Gramstad[117], F. Grancagnolo[72a], S. Grancagnolo[16], V. Grassi[148], V. Gratchev[121], N. Grau[35], H.M. Gray[30], J.A. Gray[148], E. Graziani[134a], O.G. Grebenyuk[121], T. Greenshaw[73], Z.D. Greenwood[25,l], K. Gregersen[36], I.M. Gregor[42], P. Grenier[143], J. Griffiths[8], N. Grigalashvili[64], A.A. Grillo[137], S. Grinstein[12], Ph. Gris[34], Y.V. Grishkevich[97], J.-F. Grivaz[115], E. Gross[172], J. Grosse-Knetter[54], J. Groth-Jensen[172], K. Grybel[141], D. Guest[176], C. Guicheney[34], E. Guido[50a,50b], S. Guindon[54], U. Gul[53], J. Gunther[125], B. Guo[158], J. Guo[35], P. Gutierrez[111], N. Guttman[153], O. Gutzwiller[173], C. Guyot[136], C. Gwenlan[118], C.B. Gwilliam[73], A. Haas[108], S. Haas[30], C. Haber[15], H.K. Hadavand[8], D.R. Hadley[18], P. Haefner[21], F. Hahn[30], Z. Hajduk[39], H. Hakobyan[177], D. Hall[118], K. Hamacher[175], P. Hamal[113], K. Hamano[86], M. Hamer[54], A. Hamilton[145b,o], S. Hamilton[161], L. Han[33b], K. Hanagaki[116], K. Hanawa[160], M. Hance[15], C. Handel[81], P. Hanke[58a], J.R. Hansen[36], J.B. Hansen[36], J.D. Hansen[36], P.H. Hansen[36], P. Hansson[143], K. Hara[160], T. Harenberg[175], S. Harkusha[90], D. Harper[87], R.D. Harrington[46], O.M. Harris[138], J. Hartert[48], F. Hartjes[105], T. Haruyama[65], A. Harvey[56], S. Hasegawa[101], Y. Hasegawa[140], S. Hassani[136], S. Haug[17], M. Hauschild[30], R. Hauser[88], M. Havranek[21], C.M. Hawkes[18], R.J. Hawkings[30], A.D. Hawkins[79], T. Hayakawa[66], T. Hayashi[160], D. Hayden[76], C.P. Hays[118], H.S. Hayward[73], S.J. Haywood[129], S.J. Head[18], V. Hedberg[79], L. Heelan[8], S. Heim[120], B. Heinemann[15], S. Heisterkamp[36], L. Helary[22], C. Heller[98], M. Heller[30], S. Hellman[146a,146b], D. Hellmich[21], C. Helsens[12], R.C.W. Henderson[71], M. Henke[58a], A. Henrichs[176], A.M. Henriques Correia[30], S. Henrot-Versille[115], C. Hensel[54], T. Henß[175], C.M. Hernandez[8], Y. Hernández Jiménez[167], R. Herrberg[16],

JHEP01(2013)029

G. Herten[48], R. Hertenberger[98], L. Hervas[30], G.G. Hesketh[77], N.P. Hessey[105], E. Higón-Rodriguez[167], J.C. Hill[28], K.H. Hiller[42], S. Hillert[21], S.J. Hillier[18], I. Hinchliffe[15], E. Hines[120], M. Hirose[116], F. Hirsch[43], D. Hirschbuehl[175], J. Hobbs[148], N. Hod[153], M.C. Hodgkinson[139], P. Hodgson[139], A. Hoecker[30], M.R. Hoeferkamp[103], J. Hoffman[40], D. Hoffmann[83], M. Hohlfeld[81], M. Holder[141], S.O. Holmgren[146a], T. Holy[127], J.L. Holzbauer[88], T.M. Hong[120], L. Hooft van Huysduynen[108], S. Horner[48], J-Y. Hostachy[55], S. Hou[151], A. Hoummada[135a], J. Howard[118], J. Howarth[82], I. Hristova[16], J. Hrivnac[115], T. Hryn'ova[5], P.J. Hsu[81], S.-C. Hsu[15], D. Hu[35], Z. Hubacek[127], F. Hubaut[83], F. Huegging[21], A. Huettmann[42], T.B. Huffman[118], E.W. Hughes[35], G. Hughes[71], M. Huhtinen[30], M. Hurwitz[15], N. Huseynov[64,p], J. Huston[88], J. Huth[57], G. Iacobucci[49], G. Iakovidis[10], M. Ibbotson[82], I. Ibragimov[141], L. Iconomidou-Fayard[115], J. Idarraga[115], P. Iengo[102a], O. Igonkina[105], Y. Ikegami[65], M. Ikeno[65], D. Iliadis[154], N. Ilic[158], T. Ince[99], P. Ioannou[9], M. Iodice[134a], K. Iordanidou[9], V. Ippolito[132a,132b], A. Irles Quiles[167], C. Isaksson[166], M. Ishino[67], M. Ishitsuka[157], R. Ishmukhametov[109], C. Issever[118], S. Istin[19a], A.V. Ivashin[128], W. Iwanski[39], H. Iwasaki[65], J.M. Izen[41], V. Izzo[102a], B. Jackson[120], J.N. Jackson[73], P. Jackson[1], M.R. Jaekel[30], V. Jain[60], K. Jakobs[48], S. Jakobsen[36], T. Jakoubek[125], J. Jakubek[127], D.O. Jamin[151], D.K. Jana[111], E. Jansen[77], H. Jansen[30], J. Janssen[21], A. Jantsch[99], M. Janus[48], G. Jarlskog[79], L. Jeanty[57], I. Jen-La Plante[31], D. Jennens[86], P. Jenni[30], A.E. Loevschall-Jensen[36], P. Ježˇ[36], S. Jézéquel[5], M.K. Jha[20a], H. Ji[173], W. Ji[81], J. Jia[148], Y. Jiang[33b], M. Jimenez Belenguer[42], S. Jin[33a], O. Jinnouchi[157], M.D. Joergensen[36], D. Joffe[40], M. Johansen[146a,146b], K.E. Johansson[146a], P. Johansson[139], S. Johnert[42], K.A. Johns[7], K. Jon-And[146a,146b], G. Jones[170], R.W.L. Jones[71], T.J. Jones[73], C. Joram[30], P.M. Jorge[124a], K.D. Joshi[82], J. Jovicevic[147], T. Jovin[13b], X. Ju[173], C.A. Jung[43], R.M. Jungst[30], V. Juranek[125], P. Jussel[61], A. Juste Rozas[12], S. Kabana[17], M. Kaci[167], A. Kaczmarska[39], P. Kadlecik[36], M. Kado[115], H. Kagan[109], M. Kagan[57], E. Kajomovitz[152], S. Kalinin[175], L.V. Kalinovskaya[64], S. Kama[40], N. Kanaya[155], M. Kaneda[30], S. Kaneti[28], T. Kanno[157], V.A. Kantserov[96], J. Kanzaki[65], B. Kaplan[108], A. Kapliy[31], J. Kaplon[30], D. Kar[53], M. Karagounis[21], K. Karakostas[10], M. Karnevskiy[42], V. Kartvelishvili[71], A.N. Karyukhin[128], L. Kashif[173], G. Kasieczka[58b], R.D. Kass[109], A. Kastanas[14], M. Kataoka[5], Y. Kataoka[155], E. Katsoufis[10], J. Katzy[42], V. Kaushik[7], K. Kawagoe[69], T. Kawamoto[155], G. Kawamura[81], M.S. Kayl[105], S. Kazama[155], V.A. Kazanin[107], M.Y. Kazarinov[64], R. Keeler[169], P.T. Keener[120], R. Kehoe[40], M. Keil[54], G.D. Kekelidze[64], J.S. Keller[138], M. Kenyon[53], O. Kepka[125], N. Kerschen[30], B.P. Kerševan[74], S. Kersten[175], K. Kessoku[155], J. Keung[158], F. Khalil-zada[11], H. Khandanyan[146a,146b], A. Khanov[112], D. Kharchenko[64], A. Khodinov[96], A. Khomich[58a], T.J. Khoo[28], G. Khoriauli[21], A. Khoroshilov[175], V. Khovanskiy[95], E. Khramov[64], J. Khubua[51b], H. Kim[146a,146b], S.H. Kim[160], N. Kimura[171], O. Kind[16], B.T. King[73], M. King[66], R.S.B. King[118], J. Kirk[129], A.E. Kiryunin[99], T. Kishimoto[66], D. Kisielewska[38], T. Kitamura[66], T. Kittelmann[123], K. Kiuchi[160], E. Kladiva[144b], M. Klein[73], U. Klein[73], K. Kleinknecht[81], M. Klemetti[85], A. Klier[172], P. Klimek[146a,146b], A. Klimentov[25], R. Klingenberg[43], J.A. Klinger[82], E.B. Klinkby[36], T. Klioutchnikova[30], P.F. Klok[104], S. Klous[105], E.-E. Kluge[58a], T. Kluge[73], P. Kluit[105], S. Kluth[99], E. Kneringer[61], E.B.F.G. Knoops[83], A. Knue[54], B.R. Ko[45], T. Kobayashi[155], M. Kobel[44], M. Kocian[143], P. Kodys[126], K. Köneke[30], A.C. König[104], S. Koenig[81], L. Köpke[81], F. Koetsveld[104], P. Koevesarki[21], T. Koffas[29], E. Koffeman[105], L.A. Kogan[118], S. Kohlmann[175], F. Kohn[54], Z. Kohout[127], T. Kohriki[65], T. Koi[143], G.M. Kolachev[107,*], H. Kolanoski[16], V. Kolesnikov[64], I. Koletsou[89a], J. Koll[88], A.A. Komar[94], Y. Komori[155], T. Kondo[65], T. Kono[42,q], A.I. Kononov[48], R. Konoplich[108,r], N. Konstantinidis[77], R. Kopeliansky[152], S. Koperny[38], K. Korcyl[39], K. Kordas[154], A. Korn[118], A. Korol[107], I. Korolkov[12], E.V. Korolkova[139], V.A. Korotkov[128], O. Kortner[99], S. Kortner[99], V.V. Kostyukhin[21], S. Kotov[99], V.M. Kotov[64], A. Kotwal[45], C. Kourkoumelis[9], V. Kouskoura[154],

JHEP01(2013)029

A. Koutsman[159a], R. Kowalewski[169], T.Z. Kowalski[38], W. Kozanecki[136], A.S. Kozhin[128], V. Kral[127], V.A. Kramarenko[97], G. Kramberger[74], M.W. Krasny[78], A. Krasznahorkay[108], J.K. Kraus[21], S. Kreiss[108], F. Krejci[127], J. Kretzschmar[73], N. Krieger[54], P. Krieger[158], K. Kroeninger[54], H. Kroha[99], J. Kroll[120], J. Kroseberg[21], J. Krstic[13a], U. Kruchonak[64], H. Krüger[21], T. Kruker[17], N. Krumnack[63], Z.V. Krumshteyn[64], M.K. Kruse[45], T. Kubota[86], S. Kuday[4a], S. Kuehn[48], A. Kugel[58c], T. Kuhl[42], D. Kuhn[61], V. Kukhtin[64], Y. Kulchitsky[90], S. Kuleshov[32b], C. Kummer[98], M. Kuna[78], J. Kunkle[120], A. Kupco[125], H. Kurashige[66], M. Kurata[160], Y.A. Kurochkin[90], V. Kus[125], E.S. Kuwertz[147], M. Kuze[157], J. Kvita[142], R. Kwee[16], A. La Rosa[49], L. La Rotonda[37a,37b], L. Labarga[80], J. Labbe[5], S. Lablak[135a], C. Lacasta[167], F. Lacava[132a,132b], J. Lacey[29], H. Lacker[16], D. Lacour[78], V.R. Lacuesta[167], E. Ladygin[64], R. Lafaye[5], B. Laforge[78], T. Lagouri[176], S. Lai[48], E. Laisne[55], L. Lambourne[77], C.L. Lampen[7], W. Lampl[7], E. Lancon[136], U. Landgraf[48], M.P.J. Landon[75], V.S. Lang[58a], C. Lange[42], A.J. Lankford[163], F. Lanni[25], K. Lantzsch[175], S. Laplace[78], C. Lapoire[21], J.F. Laporte[136], T. Lari[89a], A. Larner[118], M. Lassnig[30], P. Laurelli[47], V. Lavorini[37a,37b], W. Lavrijsen[15], P. Laycock[73], O. Le Dortz[78], E. Le Guirriec[83], E. Le Menedeu[12], T. LeCompte[6], F. Ledroit-Guillon[55], H. Lee[105], J.S.H. Lee[116], S.C. Lee[151], L. Lee[176], M. Lefebvre[169], M. Legendre[136], F. Legger[98], C. Leggett[15], M. Lehmacher[21], G. Lehmann Miotto[30], M.A.L. Leite[24d], R. Leitner[126], D. Lellouch[172], B. Lemmer[54], V. Lendermann[58a], K.J.C. Leney[145b], T. Lenz[105], G. Lenzen[175], B. Lenzi[30], K. Leonhardt[44], S. Leontsinis[10], F. Lepold[58a], C. Leroy[93], J-R. Lessard[169], C.G. Lester[28], C.M. Lester[120], J. Levêque[5], D. Levin[87], L.J. Levinson[172], A. Lewis[118], G.H. Lewis[108], A.M. Leyko[21], M. Leyton[16], B. Li[33b], B. Li[83], H. Li[148], H.L. Li[31], S. Li[33b,s], X. Li[87], Z. Liang[118,t], H. Liao[34], B. Liberti[133a], P. Lichard[30], M. Lichtnecker[98], K. Lie[165], W. Liebig[14], C. Limbach[21], A. Limosani[86], M. Limper[62], S.C. Lin[151,u], F. Linde[105], J.T. Linnemann[88], E. Lipeles[120], A. Lipniacka[14], T.M. Liss[165], D. Lissauer[25], A. Lister[49], A.M. Litke[137], C. Liu[29], D. Liu[151], H. Liu[87], J.B. Liu[87], L. Liu[87], M. Liu[33b], Y. Liu[33b], M. Livan[119a,119b], S.S.A. Livermore[118], A. Lleres[55], J. Llorente Merino[80], S.L. Lloyd[75], E. Lobodzinska[42], P. Loch[7], W.S. Lockman[137], T. Loddenkoetter[21], F.K. Loebinger[82], A. Loginov[176], C.W. Loh[168], T. Lohse[16], K. Lohwasser[48], M. Lokajicek[125], V.P. Lombardo[5], R.E. Long[71], L. Lopes[124a], D. Lopez Mateos[57], J. Lorenz[98], N. Lorenzo Martinez[115], M. Losada[162], P. Loscutoff[15], F. Lo Sterzo[132a,132b], M.J. Losty[159a,*], X. Lou[41], A. Lounis[115], K.F. Loureiro[162], J. Love[6], P.A. Love[71], A.J. Lowe[143,e], F. Lu[33a], H.J. Lubatti[138], C. Luci[132a,132b], A. Lucotte[55], A. Ludwig[44], D. Ludwig[42], I. Ludwig[48], J. Ludwig[48], F. Luehring[60], G. Luijckx[105], W. Lukas[61], L. Luminari[132a], E. Lund[117], B. Lund-Jensen[147], B. Lundberg[79], J. Lundberg[146a,146b], O. Lundberg[146a,146b], J. Lundquist[36], M. Lungwitz[81], D. Lynn[25], E. Lytken[79], H. Ma[25], L.L. Ma[173], G. Maccarrone[47], A. Macchiolo[99], B. Maček[74], J. Machado Miguens[124a], D. Macina[30], R. Mackeprang[36], R.J. Madaras[15], H.J. Maddocks[71], W.F. Mader[44], R. Maenner[58c], T. Maeno[25], P. Mättig[175], S. Mättig[42], L. Magnoni[163], E. Magradze[54], K. Mahboubi[48], J. Mahlstedt[105], S. Mahmoud[73], G. Mahout[18], C. Maiani[136], C. Maidantchik[24a], A. Maio[124a,b], S. Majewski[25], Y. Makida[65], N. Makovec[115], P. Mal[136], B. Malaescu[30], Pa. Malecki[39], P. Malecki[39], V.P. Maleev[121], F. Malek[55], U. Mallik[62], D. Malon[6], C. Malone[143], S. Maltezos[10], V. Malyshev[107], S. Malyukov[30], R. Mameghani[98], J. Mamuzic[13b], A. Manabe[65], L. Mandelli[89a], I. Mandić[74], R. Mandrysch[16], J. Maneira[124a], A. Manfredini[99], L. Manhaes de Andrade Filho[24b], J.A. Manjarres Ramos[136], A. Mann[54], P.M. Manning[137], A. Manousakis-Katsikakis[9], B. Mansoulie[136], A. Mapelli[30], L. Mapelli[30], L. March[167], J.F. Marchand[29], F. Marchese[133a,133b], G. Marchiori[78], M. Marcisovsky[125], C.P. Marino[169], F. Marroquim[24a], Z. Marshall[30], L.F. Marti[17], S. Marti-Garcia[167], B. Martin[30], B. Martin[88], J.P. Martin[93], T.A. Martin[18], V.J. Martin[46], B. Martin dit Latour[49], S. Martin-Haugh[149], M. Martinez[12], V. Martinez Outschoorn[57], A.C. Martyniuk[169], M. Marx[82], F. Marzano[132a], A. Marzin[111],

JHEP01(2013)029

L. Masetti[81], T. Mashimo[155], R. Mashinistov[94], J. Masik[82], A.L. Maslennikov[107], I. Massa[20a,20b], G. Massaro[105], N. Massol[5], P. Mastrandrea[148], A. Mastroberardino[37a,37b], T. Masubuchi[155], P. Matricon[115], H. Matsunaga[155], T. Matsushita[66], C. Mattravers[118,c], J. Maurer[83], S.J. Maxfield[73], D.A. Maximov[107,f], A. Mayne[139], R. Mazini[151], M. Mazur[21], L. Mazzaferro[133a,133b], M. Mazzanti[89a], J. Mc Donald[85], S.P. Mc Kee[87], A. McCarn[165], R.L. McCarthy[148], T.G. McCarthy[29], N.A. McCubbin[129], K.W. McFarlane[56,*], J.A. Mcfayden[139], G. Mchedlidze[51b], T. Mclaughlan[18], S.J. McMahon[129], R.A. McPherson[169,j], A. Meade[84], J. Mechnich[105], M. Mechtel[175], M. Medinnis[42], S. Meehan[31], R. Meera-Lebbai[111], T. Meguro[116], S. Mehlhase[36], A. Mehta[73], K. Meier[58a], B. Meirose[79], C. Melachrinos[31], B.R. Mellado Garcia[173], F. Meloni[89a,89b], L. Mendoza Navas[162], Z. Meng[151,v], A. Mengarelli[20a,20b], S. Menke[99], E. Meoni[161], K.M. Mercurio[57], P. Mermod[49], L. Merola[102a,102b], C. Meroni[89a], F.S. Merritt[31], H. Merritt[109], A. Messina[30,w], J. Metcalfe[25], A.S. Mete[163], C. Meyer[81], C. Meyer[31], J-P. Meyer[136], J. Meyer[174], J. Meyer[54], S. Michal[30], L. Micu[26a], R.P. Middleton[129], S. Migas[73], L. Mijović[136], G. Mikenberg[172], M. Mikestikova[125], M. Mikuž[74], D.W. Miller[31], R.J. Miller[88], W.J. Mills[168], C. Mills[57], A. Milov[172], D.A. Milstead[146a,146b], D. Milstein[172], A.A. Minaenko[128], M. Miñano Moya[167], I.A. Minashvili[64], A.I. Mincer[108], B. Mindur[38], M. Mineev[64], Y. Ming[173], L.M. Mir[12], G. Mirabelli[132a], J. Mitrevski[137], V.A. Mitsou[167], S. Mitsui[65], P.S. Miyagawa[139], J.U. Mjörnmark[79], T. Moa[146a,146b], V. Moeller[28], K. Mönig[42], N. Möser[21], S. Mohapatra[148], W. Mohr[48], R. Moles-Valls[167], A. Molfetas[30], J. Monk[77], E. Monnier[83], J. Montejo Berlingen[12], F. Monticelli[70], S. Monzani[20a,20b], R.W. Moore[3], G.F. Moorhead[86], C. Mora Herrera[49], A. Moraes[53], N. Morange[136], J. Morel[54], G. Morello[37a,37b], D. Moreno[81], M. Moreno Llácer[167], P. Morettini[50a], M. Morgenstern[44], M. Morii[57], A.K. Morley[30], G. Mornacchi[30], J.D. Morris[75], L. Morvaj[101], H.G. Moser[99], M. Mosidze[51b], J. Moss[109], R. Mount[143], E. Mountricha[10,x], S.V. Mouraviev[94,*], E.J.W. Moyse[84], F. Mueller[58a], J. Mueller[123], K. Mueller[21], T.A. Müller[98], T. Mueller[81], D. Muenstermann[30], Y. Munwes[153], W.J. Murray[129], I. Mussche[105], E. Musto[152], A.G. Myagkov[128], M. Myska[125], O. Nackenhorst[54], J. Nadal[12], K. Nagai[160], R. Nagai[157], K. Nagano[65], A. Nagarkar[109], Y. Nagasaka[59], M. Nagel[99], A.M. Nairz[30], Y. Nakahama[30], K. Nakamura[155], T. Nakamura[155], I. Nakano[110], G. Nanava[21], A. Napier[161], R. Narayan[58b], M. Nash[77,c], T. Nattermann[21], T. Naumann[42], G. Navarro[162], H.A. Neal[87], P.Yu. Nechaeva[94], T.J. Neep[82], A. Negri[119a,119b], G. Negri[30], M. Negrini[20a], S. Nektarijevic[49], A. Nelson[163], T.K. Nelson[143], S. Nemecek[125], P. Nemethy[108], A.A. Nepomuceno[24a], M. Nessi[30,y], M.S. Neubauer[165], M. Neumann[175], A. Neusiedl[81], R.M. Neves[108], P. Nevski[25], F.M. Newcomer[120], P.R. Newman[18], V. Nguyen Thi Hong[136], R.B. Nickerson[118], R. Nicolaidou[136], B. Nicquevert[30], F. Niedercorn[115], J. Nielsen[137], N. Nikiforou[35], A. Nikiforov[16], V. Nikolaenko[128], I. Nikolic-Audit[78], K. Nikolics[49], K. Nikolopoulos[18], H. Nilsen[48], P. Nilsson[8], Y. Ninomiya[155], A. Nisati[132a], R. Nisius[99], T. Nobe[157], L. Nodulman[6], M. Nomachi[116], I. Nomidis[154], S. Norberg[111], M. Nordberg[30], P.R. Norton[129], J. Novakova[126], M. Nozaki[65], L. Nozka[113], I.M. Nugent[159a], A.-E. Nuncio-Quiroz[21], G. Nunes Hanninger[86], T. Nunnemann[98], E. Nurse[77], B.J. O'Brien[46], D.C. O'Neil[142], V. O'Shea[53], L.B. Oakes[98], F.G. Oakham[29,d], H. Oberlack[99], J. Ocariz[78], A. Ochi[66], S. Oda[69], S. Odaka[65], J. Odier[83], H. Ogren[60], A. Oh[82], S.H. Oh[45], C.C. Ohm[30], T. Ohshima[101], W. Okamura[116], H. Okawa[25], Y. Okumura[31], T. Okuyama[155], A. Olariu[26a], A.G. Olchevski[64], S.A. Olivares Pino[32a], M. Oliveira[124a,g], D. Oliveira Damazio[25], E. Oliver Garcia[167], D. Olivito[120], A. Olszewski[39], J. Olszowska[39], A. Onofre[124a,z], P.U.E. Onyisi[31], C.J. Oram[159a], M.J. Oreglia[31], Y. Oren[153], D. Orestano[134a,134b], N. Orlando[72a,72b], I. Orlov[107], C. Oropeza Barrera[53], R.S. Orr[158], B. Osculati[50a,50b], R. Ospanov[120], C. Osuna[12], G. Otero y Garzon[27], J.P. Ottersbach[105], M. Ouchrif[135d], E.A. Ouellette[169], F. Ould-Saada[117], A. Ouraou[136], Q. Ouyang[33a], A. Ovcharova[15], M. Owen[82], S. Owen[139],

JHEP01(2013)029

V.E. Ozcan[19a], N. Ozturk[8], A. Pacheco Pages[12], C. Padilla Aranda[12], S. Pagan Griso[15], E. Paganis[139], C. Pahl[99], F. Paige[25], P. Pais[84], K. Pajchel[117], G. Palacino[159b], C.P. Paleari[7], S. Palestini[30], D. Pallin[34], A. Palma[124a], J.D. Palmer[18], Y.B. Pan[173], E. Panagiotopoulou[10], J.G. Panduro Vazquez[76], P. Pani[105], N. Panikashvili[87], S. Panitkin[25], D. Pantea[26a], A. Papadelis[146a], Th.D. Papadopoulou[10], A. Paramonov[6], D. Paredes Hernandez[34], W. Park[25,aa], M.A. Parker[28], F. Parodi[50a,50b], J.A. Parsons[35], U. Parzefall[48], S. Pashapour[54], E. Pasqualucci[132a], S. Passaggio[50a], A. Passeri[134a], F. Pastore[134a,134b,*], Fr. Pastore[76], G. Pásztor[49,ab], S. Pataraia[175], N. Patel[150], J.R. Pater[82], S. Patricelli[102a,102b], T. Pauly[30], M. Pecsy[144a], S. Pedraza Lopez[167], M.I. Pedraza Morales[173], S.V. Peleganchuk[107], D. Pelikan[166], H. Peng[33b], B. Penning[31], A. Penson[35], J. Penwell[60], M. Perantoni[24a], K. Perez[35,ac], T. Perez Cavalcanti[42], E. Perez Codina[159a], M.T. Pérez García-Estañ[167], V. Perez Reale[35], L. Perini[89a,89b], H. Pernegger[30], R. Perrino[72a], P. Perrodo[5], V.D. Peshekhonov[64], K. Peters[30], B.A. Petersen[30], J. Petersen[30], T.C. Petersen[36], E. Petit[5], A. Petridis[154], C. Petridou[154], E. Petrolo[132a], F. Petrucci[134a,134b], D. Petschull[42], M. Petteni[142], R. Pezoa[32b], A. Phan[86], P.W. Phillips[129], G. Piacquadio[30], A. Picazio[49], E. Piccaro[75], M. Piccinini[20a,20b], S.M. Piec[42], R. Piegaia[27], D.T. Pignotti[109], J.E. Pilcher[31], A.D. Pilkington[82], J. Pina[124a,b], M. Pinamonti[164a,164c], A. Pinder[118], J.L. Pinfold[3], B. Pinto[124a], C. Pizio[89a,89b], M. Plamondon[169], M.-A. Pleier[25], E. Plotnikova[64], A. Poblaguev[25], S. Poddar[58a], F. Podlyski[34], L. Poggioli[115], D. Pohl[21], M. Pohl[49], G. Polesello[119a], A. Policicchio[37a,37b], A. Polini[20a], J. Poll[75], V. Polychronakos[25], D. Pomeroy[23], K. Pommès[30], L. Pontecorvo[132a], B.G. Pope[88], G.A. Popeneciu[26a], D.S. Popovic[13a], A. Poppleton[30], X. Portell Bueso[30], G.E. Pospelov[99], S. Pospisil[127], I.N. Potrap[99], C.J. Potter[149], C.T. Potter[114], G. Poulard[30], J. Poveda[60], V. Pozdnyakov[64], R. Prabhu[77], P. Pralavorio[83], A. Pranko[15], S. Prasad[30], R. Pravahan[25], S. Prell[63], K. Pretzl[17], D. Price[60], J. Price[73], L.E. Price[6], D. Prieur[123], M. Primavera[72a], K. Prokofiev[108], F. Prokoshin[32b], S. Protopopescu[25], J. Proudfoot[6], X. Prudent[44], M. Przybycien[38], H. Przysiezniak[5], S. Psoroulas[21], E. Ptacek[114], E. Pueschel[84], J. Purdham[87], M. Purohit[25,aa], P. Puzo[115], Y. Pylypchenko[62], J. Qian[87], A. Quadt[54], D.R. Quarrie[15], W.B. Quayle[173], F. Quinonez[32a], M. Raas[104], V. Radeka[25], V. Radescu[42], P. Radloff[114], F. Ragusa[89a,89b], G. Rahal[178], A.M. Rahimi[109], D. Rahm[25], S. Rajagopalan[25], M. Rammensee[48], M. Rammes[141], A.S. Randle-Conde[40], K. Randrianarivony[29], F. Rauscher[98], T.C. Rave[48], M. Raymond[30], A.L. Read[117], D.M. Rebuzzi[119a,119b], A. Redelbach[174], G. Redlinger[25], R. Reece[120], K. Reeves[41], A. Reinsch[114], I. Reisinger[43], C. Rembser[30], Z.L. Ren[151], A. Renaud[115], M. Rescigno[132a], S. Resconi[89a], B. Resende[136], P. Reznicek[98], R. Rezvani[158], R. Richter[99], E. Richter-Was[5,ad], M. Ridel[78], M. Rijpstra[105], M. Rijssenbeek[148], A. Rimoldi[119a,119b], L. Rinaldi[20a], R.R. Rios[40], I. Riu[12], G. Rivoltella[89a,89b], F. Rizatdinova[112], E. Rizvi[75], S.H. Robertson[85,j], A. Robichaud-Veronneau[118], D. Robinson[28], J.E.M. Robinson[82], A. Robson[53], J.G. Rocha de Lima[106], C. Roda[122a,122b], D. Roda Dos Santos[30], A. Roe[54], S. Roe[30], O. Røhne[117], S. Rolli[161], A. Romaniouk[96], M. Romano[20a,20b], G. Romeo[27], E. Romero Adam[167], N. Rompotis[138], L. Roos[78], E. Ros[167], S. Rosati[132a], K. Rosbach[49], A. Rose[149], M. Rose[76], G.A. Rosenbaum[158], E.I. Rosenberg[63], P.L. Rosendahl[14], O. Rosenthal[141], L. Rosselet[49], V. Rossetti[12], E. Rossi[132a,132b], L.P. Rossi[50a], M. Rotaru[26a], I. Roth[172], J. Rothberg[138], D. Rousseau[115], C.R. Royon[136], A. Rozanov[83], Y. Rozen[152], X. Ruan[33a,ae], F. Rubbo[12], I. Rubinskiy[42], N. Ruckstuhl[105], V.I. Rud[97], C. Rudolph[44], G. Rudolph[61], F. Rühr[7], A. Ruiz-Martinez[63], L. Rumyantsev[64], Z. Rurikova[48], N.A. Rusakovich[64], A. Ruschke[98], J.P. Rutherfoord[7], P. Ruzicka[125], Y.F. Ryabov[121], M. Rybar[126], G. Rybkin[115], N.C. Ryder[118], A.F. Saavedra[150], I. Sadeh[153], H.F-W. Sadrozinski[137], R. Sadykov[64], F. Safai Tehrani[132a], H. Sakamoto[155], G. Salamanna[75], A. Salamon[133a], M. Saleem[111], D. Salek[30], D. Salihagic[99], A. Salnikov[143], J. Salt[167], B.M. Salvachua Ferrando[6], D. Salvatore[37a,37b], F. Salvatore[149],

JHEP01(2013)029

A. Salvucci[104], A. Salzburger[30], D. Sampsonidis[154], B.H. Samset[117], A. Sanchez[102a,102b], V. Sanchez Martinez[167], H. Sandaker[14], H.G. Sander[81], M.P. Sanders[98], M. Sandhoff[175], T. Sandoval[28], C. Sandoval[162], R. Sandstroem[99], D.P.C. Sankey[129], A. Sansoni[47], C. Santamarina Rios[85], C. Santoni[34], R. Santonico[133a,133b], H. Santos[124a], I. Santoyo Castillo[149], J.G. Saraiva[124a], T. Sarangi[173], E. Sarkisyan-Grinbaum[8], F. Sarri[122a,122b], G. Sartisohn[175], O. Sasaki[65], Y. Sasaki[155], N. Sasao[67], I. Satsounkevitch[90], G. Sauvage[5,*], E. Sauvan[5], J.B. Sauvan[115], P. Savard[158,d], V. Savinov[123], D.O. Savu[30], L. Sawyer[25,l], D.H. Saxon[53], J. Saxon[120], C. Sbarra[20a], A. Sbrizzi[20a,20b], D.A. Scannicchio[163], M. Scarcella[150], J. Schaarschmidt[115], P. Schacht[99], D. Schaefer[120], U. Schäfer[81], A. Schaelicke[46], S. Schaepe[21], S. Schaetzel[58b], A.C. Schaffer[115], D. Schaile[98], R.D. Schamberger[148], A.G. Schamov[107], V. Scharf[58a], V.A. Schegelsky[121], D. Scheirich[87], M. Schernau[163], M.I. Scherzer[35], C. Schiavi[50a,50b], J. Schieck[98], M. Schioppa[37a,37b], S. Schlenker[30], E. Schmidt[48], K. Schmieden[21], C. Schmitt[81], S. Schmitt[58b], B. Schneider[17], U. Schnoor[44], L. Schoeffel[136], A. Schoening[58b], A.L.S. Schorlemmer[54], M. Schott[30], D. Schouten[159a], J. Schovancova[125], M. Schram[85], C. Schroeder[81], N. Schroer[58c], M.J. Schultens[21], J. Schultes[175], H.-C. Schultz-Coulon[58a], H. Schulz[16], M. Schumacher[48], B.A. Schumm[137], Ph. Schune[136], C. Schwanenberger[82], A. Schwartzman[143], Ph. Schwegler[99], Ph. Schwemling[78], R. Schwienhorst[88], R. Schwierz[44], J. Schwindling[136], T. Schwindt[21], M. Schwoerer[5], F.G. Sciacca[17], G. Sciolla[23], W.G. Scott[129], J. Searcy[114], G. Sedov[42], E. Sedykh[121], S.C. Seidel[103], A. Seiden[137], F. Seifert[44], J.M. Seixas[24a], G. Sekhniaidze[102a], S.J. Sekula[40], K.E. Selbach[46], D.M. Seliverstov[121], B. Sellden[146a], G. Sellers[73], M. Seman[144b], N. Semprini-Cesari[20a,20b], C. Serfon[98], L. Serin[115], L. Serkin[54], R. Seuster[159a], H. Severini[111], A. Sfyrla[30], E. Shabalina[54], M. Shamim[114], L.Y. Shan[33a], J.T. Shank[22], Q.T. Shao[86], M. Shapiro[15], P.B. Shatalov[95], K. Shaw[164a,164c], D. Sherman[176], P. Sherwood[77], S. Shimizu[101], M. Shimojima[100], T. Shin[56], M. Shiyakova[64], A. Shmeleva[94], M.J. Shochet[31], D. Short[118], S. Shrestha[63], E. Shulga[96], M.A. Shupe[7], P. Sicho[125], A. Sidoti[132a], F. Siegert[48], Dj. Sijacki[13a], O. Silbert[172], J. Silva[124a], Y. Silver[153], D. Silverstein[143], S.B. Silverstein[146a], V. Simak[127], O. Simard[136], Lj. Simic[13a], S. Simion[115], E. Simioni[81], B. Simmons[77], R. Simoniello[89a,89b], M. Simonyan[36], P. Sinervo[158], N.B. Sinev[114], V. Sipica[141], G. Siragusa[174], A. Sircar[25], A.N. Sisakyan[64,*], S.Yu. Sivoklokov[97], J. Sjölin[146a,146b], T.B. Sjursen[14], L.A. Skinnari[15], H.P. Skottowe[57], K. Skovpen[107], P. Skubic[111], M. Slater[18], T. Slavicek[127], K. Sliwa[161], V. Smakhtin[172], B.H. Smart[46], L. Smestad[117], S.Yu. Smirnov[96], Y. Smirnov[96], L.N. Smirnova[97], O. Smirnova[79], B.C. Smith[57], D. Smith[143], K.M. Smith[53], M. Smizanska[71], K. Smolek[127], A.A. Snesarev[94], S.W. Snow[82], J. Snow[111], S. Snyder[25], R. Sobie[169,j], J. Sodomka[127], A. Soffer[153], C.A. Solans[167], M. Solar[127], J. Solc[127], E.Yu. Soldatov[96], U. Soldevila[167], E. Solfaroli Camillocci[132a,132b], A.A. Solodkov[128], O.V. Solovyanov[128], V. Solovyev[121], N. Soni[1], V. Sopko[127], B. Sopko[127], M. Sosebee[8], R. Soualah[164a,164c], A. Soukharev[107], S. Spagnolo[72a,72b], F. Spanò[76], R. Spighi[20a], G. Spigo[30], R. Spiwoks[30], M. Spousta[126,af], T. Spreitzer[158], B. Spurlock[8], R.D. St. Denis[53], J. Stahlman[120], R. Stamen[58a], E. Stanecka[39], R.W. Stanek[6], C. Stanescu[134a], M. Stanescu-Bellu[42], M.M. Stanitzki[42], S. Stapnes[117], E.A. Starchenko[128], J. Stark[55], P. Staroba[125], P. Starovoitov[42], R. Staszewski[39], A. Staude[98], P. Stavina[144a,*], G. Steele[53], P. Steinbach[44], P. Steinberg[25], I. Stekl[127], B. Stelzer[142], H.J. Stelzer[88], O. Stelzer-Chilton[159a], H. Stenzel[52], S. Stern[99], G.A. Stewart[30], J.A. Stillings[21], M.C. Stockton[85], K. Stoerig[48], G. Stoicea[26a], S. Stonjek[99], P. Strachota[126], A.R. Stradling[8], A. Straessner[44], J. Strandberg[147], S. Strandberg[146a,146b], A. Strandlie[117], M. Strang[109], E. Strauss[143], M. Strauss[111], P. Strizenec[144b], R. Ströhmer[174], D.M. Strom[114], J.A. Strong[76,*], R. Stroynowski[40], B. Stugu[14], I. Stumer[25,*], J. Stupak[148], P. Sturm[175], N.A. Styles[42], D.A. Soh[151,t], D. Su[143], HS. Subramania[3], R. Subramaniam[25], A. Succurro[12], Y. Sugaya[116], C. Suhr[106],

JHEP01(2013)029

M. Suk[126], V.V. Sulin[94], S. Sultansoy[4d], T. Sumida[67], X. Sun[55], J.E. Sundermann[48], K. Suruliz[139], G. Susinno[37a,37b], M.R. Sutton[149], Y. Suzuki[65], Y. Suzuki[66], M. Svatos[125], S. Swedish[168], I. Sykora[144a], T. Sykora[126], J. Sánchez[167], D. Ta[105], K. Tackmann[42], A. Taffard[163], R. Tafirout[159a], N. Taiblum[153], Y. Takahashi[101], H. Takai[25], R. Takashima[68], H. Takeda[66], T. Takeshita[140], Y. Takubo[65], M. Talby[83], A. Talyshev[107,f], M.C. Tamsett[25], K.G. Tan[86], J. Tanaka[155], R. Tanaka[115], S. Tanaka[131], S. Tanaka[65], A.J. Tanasijczuk[142], K. Tani[66], N. Tannoury[83], S. Tapprogge[81], D. Tardif[158], S. Tarem[152], F. Tarrade[29], G.F. Tartarelli[89a], P. Tas[126], M. Tasevsky[125], E. Tassi[37a,37b], Y. Tayalati[135d], C. Taylor[77], F.E. Taylor[92], G.N. Taylor[86], W. Taylor[159b], M. Teinturier[115], F.A. Teischinger[30], M. Teixeira Dias Castanheira[75], P. Teixeira-Dias[76], K.K. Temming[48], H. Ten Kate[30], P.K. Teng[151], S. Terada[65], K. Terashi[155], J. Terron[80], M. Testa[47], R.J. Teuscher[158,j], J. Therhaag[21], T. Theveneaux-Pelzer[78], S. Thoma[48], J.P. Thomas[18], E.N. Thompson[35], P.D. Thompson[18], P.D. Thompson[158], A.S. Thompson[53], L.A. Thomsen[36], E. Thomson[120], M. Thomson[28], W.M. Thong[86], R.P. Thun[87], F. Tian[35], M.J. Tibbetts[15], T. Tic[125], V.O. Tikhomirov[94], Y.A. Tikhonov[107,f], S. Timoshenko[96], E. Tiouchichine[83], P. Tipton[176], S. Tisserant[83], T. Todorov[5], S. Todorova-Nova[161], B. Toggerson[163], J. Tojo[69], S. Tokár[144a], K. Tokushuku[65], K. Tollefson[88], M. Tomoto[101], L. Tompkins[31], K. Toms[103], A. Tonoyan[14], C. Topfel[17], N.D. Topilin[64], E. Torrence[114], H. Torres[78], E. Torró Pastor[167], J. Toth[83,ab], F. Touchard[83], D.R. Tovey[139], T. Trefzger[174], L. Tremblet[30], A. Tricoli[30], I.M. Trigger[159a], S. Trincaz-Duvoid[78], M.F. Tripiana[70], N. Triplett[25], W. Trischuk[158], B. Trocmé[55], C. Troncon[89a], M. Trottier-McDonald[142], P. True[88], M. Trzebinski[39], A. Trzupek[39], C. Tsarouchas[30], J.C-L. Tseng[118], M. Tsiakiris[105], P.V. Tsiareshka[90], D. Tsionou[5,ag], G. Tsipolitis[10], S. Tsiskaridze[12], V. Tsiskaridze[48], E.G. Tskhadadze[51a], I.I. Tsukerman[95], V. Tsulaia[15], J.-W. Tsung[21], S. Tsuno[65], D. Tsybychev[148], A. Tua[139], A. Tudorache[26a], V. Tudorache[26a], J.M. Tuggle[31], M. Turala[39], D. Turecek[127], I. Turk Cakir[4e], E. Turlay[105], R. Turra[89a,89b], P.M. Tuts[35], A. Tykhonov[74], M. Tylmad[146a,146b], M. Tyndel[129], G. Tzanakos[9], K. Uchida[21], I. Ueda[155], R. Ueno[29], M. Ugland[14], M. Uhlenbrock[21], M. Uhrmacher[54], F. Ukegawa[160], G. Unal[30], A. Undrus[25], G. Unel[163], Y. Unno[65], D. Urbaniec[35], P. Urquijo[21], G. Usai[8], M. Uslenghi[119a,119b], L. Vacavant[83], V. Vacek[127], B. Vachon[85], S. Vahsen[15], J. Valenta[125], S. Valentinetti[20a,20b], A. Valero[167], S. Valkar[126], E. Valladolid Gallego[167], S. Vallecorsa[152], J.A. Valls Ferrer[167], R. Van Berg[120], P.C. Van Der Deijl[105], R. van der Geer[105], H. van der Graaf[105], R. Van Der Leeuw[105], E. van der Poel[105], D. van der Ster[30], N. van Eldik[30], P. van Gemmeren[6], I. van Vulpen[105], M. Vanadia[99], W. Vandelli[30], A. Vaniachine[6], P. Vankov[42], F. Vannucci[78], R. Vari[132a], E.W. Varnes[7], T. Varol[84], D. Varouchas[15], A. Vartapetian[8], K.E. Varvell[150], V.I. Vassilakopoulos[56], F. Vazeille[34], T. Vazquez Schroeder[54], G. Vegni[89a,89b], J.J. Veillet[115], F. Veloso[124a], R. Veness[30], S. Veneziano[132a], A. Ventura[72a,72b], D. Ventura[84], M. Venturi[48], N. Venturi[158], V. Vercesi[119a], M. Verducci[138], W. Verkerke[105], J.C. Vermeulen[105], A. Vest[44], M.C. Vetterli[142,d], I. Vichou[165], T. Vickey[145b,ah], O.E. Vickey Boeriu[145b], G.H.A. Viehhauser[118], S. Viel[168], M. Villa[20a,20b], M. Villaplana Perez[167], E. Vilucchi[47], M.G. Vincter[29], E. Vinek[30], V.B. Vinogradov[64], M. Virchaux[136,*], J. Virzi[15], O. Vitells[172], M. Viti[42], I. Vivarelli[48], F. Vives Vaque[3], S. Vlachos[10], D. Vladoiu[98], M. Vlasak[127], A. Vogel[21], P. Vokac[127], G. Volpi[47], M. Volpi[86], G. Volpini[89a], H. von der Schmitt[99], H. von Radziewski[48], E. von Toerne[21], V. Vorobel[126], V. Vorwerk[12], M. Vos[167], R. Voss[30], T.T. Voss[175], J.H. Vossebeld[73], N. Vranjes[136], M. Vranjes Milosavljevic[105], V. Vrba[125], M. Vreeswijk[105], T. Vu Anh[48], R. Vuillermet[30], I. Vukotic[31], W. Wagner[175], P. Wagner[120], H. Wahlen[175], S. Wahrmund[44], J. Wakabayashi[101], S. Walch[87], J. Walder[71], R. Walker[98], W. Walkowiak[141], R. Wall[176], P. Waller[73], B. Walsh[176], C. Wang[45], H. Wang[173], H. Wang[40], J. Wang[151], J. Wang[55], R. Wang[103], S.M. Wang[151], T. Wang[21],

JHEP01(2013)029

A. Warburton[85], C.P. Ward[28], D.R. Wardrope[77], M. Warsinsky[48], A. Washbrook[46], C. Wasicki[42], I. Watanabe[66], P.M. Watkins[18], A.T. Watson[18], I.J. Watson[150], M.F. Watson[18], G. Watts[138], S. Watts[82], A.T. Waugh[150], B.M. Waugh[77], M.S. Weber[17], J.S. Webster[31], A.R. Weidberg[118], P. Weigell[99], J. Weingarten[54], C. Weiser[48], P.S. Wells[30], T. Wenaus[25], D. Wendland[16], Z. Weng[151,t], T. Wengler[30], S. Wenig[30], N. Wermes[21], M. Werner[48], P. Werner[30], M. Werth[163], M. Wessels[58a], J. Wetter[161], C. Weydert[55], K. Whalen[29], A. White[8], M.J. White[86], S. White[122a,122b], S.R. Whitehead[118], D. Whiteson[163], D. Whittington[60], F. Wicek[115], D. Wicke[175], F.J. Wickens[129], W. Wiedenmann[173], M. Wielers[129], P. Wienemann[21], C. Wiglesworth[75], L.A.M. Wiik-Fuchs[21], P.A. Wijeratne[77], A. Wildauer[99], M.A. Wildt[42,q], I. Wilhelm[126], H.G. Wilkens[30], J.Z. Will[98], E. Williams[35], H.H. Williams[120], W. Willis[35], S. Willocq[84], J.A. Wilson[18], M.G. Wilson[143], A. Wilson[87], I. Wingerter-Seez[5], S. Winkelmann[48], F. Winklmeier[30], M. Wittgen[143], S.J. Wollstadt[81], M.W. Wolter[39], H. Wolters[124a,g], W.C. Wong[41], G. Wooden[87], B.K. Wosiek[39], J. Wotschack[30], M.J. Woudstra[82], K.W. Wozniak[39], K. Wraight[53], M. Wright[53], B. Wrona[73], S.L. Wu[173], X. Wu[49], Y. Wu[33b,ai], E. Wulf[35], B.M. Wynne[46], S. Xella[36], M. Xiao[136], S. Xie[48], C. Xu[33b,x], D. Xu[139], L. Xu[33b], B. Yabsley[150], S. Yacoob[145a,aj], M. Yamada[65], H. Yamaguchi[155], A. Yamamoto[65], K. Yamamoto[63], S. Yamamoto[155], T. Yamamura[155], T. Yamanaka[155], T. Yamazaki[155], Y. Yamazaki[66], Z. Yan[22], H. Yang[87], U.K. Yang[82], Y. Yang[109], Z. Yang[146a,146b], S. Yanush[91], L. Yao[33a], Y. Yao[15], Y. Yasu[65], G.V. Ybeles Smit[130], J. Ye[40], S. Ye[25], M. Yilmaz[4c], R. Yoosoofmiya[123], K. Yorita[171], R. Yoshida[6], K. Yoshihara[155], C. Young[143], C.J. Young[118], S. Youssef[22], D. Yu[25], J. Yu[8], J. Yu[112], L. Yuan[66], A. Yurkewicz[106], B. Zabinski[39], R. Zaidan[62], A.M. Zaitsev[128], Z. Zajacova[30], L. Zanello[132a,132b], D. Zanzi[99], A. Zaytsev[25], C. Zeitnitz[175], M. Zeman[125], A. Zemla[39], C. Zendler[21], O. Zenin[128], T. Ženiš[144a], Z. Zinonos[122a,122b], D. Zerwas[115], G. Zevi della Porta[57], D. Zhang[33b,ak], H. Zhang[88], J. Zhang[6], X. Zhang[33d], Z. Zhang[115], L. Zhao[108], Z. Zhao[33b], A. Zhemchugov[64], J. Zhong[118], B. Zhou[87], N. Zhou[163], Y. Zhou[151], C.G. Zhu[33d], H. Zhu[42], J. Zhu[87], Y. Zhu[33b], X. Zhuang[98], V. Zhuravlov[99], A. Zibell[98], D. Zieminska[60], N.I. Zimin[64], R. Zimmermann[21], S. Zimmermann[21], S. Zimmermann[48], M. Ziolkowski[141], R. Zitoun[5], L. Živković[35], V.V. Zmouchko[128,*], G. Zobernig[173], A. Zoccoli[20a,20b], M. zur Nedden[16], V. Zutshi[106], L. Zwalinski[30]

[1] School of Chemistry and Physics, University of Adelaide, Adelaide, Australia
[2] Physics Department, SUNY Albany, Albany NY, United States of America
[3] Department of Physics, University of Alberta, Edmonton AB, Canada
[4] [(a)] Department of Physics, Ankara University, Ankara; [(b)] Department of Physics, Dumlupinar University, Kutahya; [(c)] Department of Physics, Gazi University, Ankara; [(d)] Division of Physics, TOBB University of Economics and Technology, Ankara; [(e)] Turkish Atomic Energy Authority, Ankara, Turkey
[5] LAPP, CNRS/IN2P3 and Université de Savoie, Annecy-le-Vieux, France
[6] High Energy Physics Division, Argonne National Laboratory, Argonne IL, United States of America
[7] Department of Physics, University of Arizona, Tucson AZ, United States of America
[8] Department of Physics, The University of Texas at Arlington, Arlington TX, United States of America
[9] Physics Department, University of Athens, Athens, Greece
[10] Physics Department, National Technical University of Athens, Zografou, Greece
[11] Institute of Physics, Azerbaijan Academy of Sciences, Baku, Azerbaijan
[12] Institut de Física d'Altes Energies and Departament de Física de la Universitat Autònoma de Barcelona and ICREA, Barcelona, Spain
[13] [(a)] Institute of Physics, University of Belgrade, Belgrade; [(b)] Vinca Institute of Nuclear Sciences, University of Belgrade, Belgrade, Serbia
[14] Department for Physics and Technology, University of Bergen, Bergen, Norway

JHEP01(2013)029

[15] Physics Division, Lawrence Berkeley National Laboratory and University of California, Berkeley CA, United States of America
[16] Department of Physics, Humboldt University, Berlin, Germany
[17] Albert Einstein Center for Fundamental Physics and Laboratory for High Energy Physics, University of Bern, Bern, Switzerland
[18] School of Physics and Astronomy, University of Birmingham, Birmingham, United Kingdom
[19] [(a)] Department of Physics, Bogazici University, Istanbul; [(b)] Division of Physics, Dogus University, Istanbul; [(c)] Department of Physics Engineering, Gaziantep University, Gaziantep; [(d)] Department of Physics, Istanbul Technical University, Istanbul, Turkey
[20] [(a)] INFN Sezione di Bologna; [(b)] Dipartimento di Fisica, Università di Bologna, Bologna, Italy
[21] Physikalisches Institut, University of Bonn, Bonn, Germany
[22] Department of Physics, Boston University, Boston MA, United States of America
[23] Department of Physics, Brandeis University, Waltham MA, United States of America
[24] [(a)] Universidade Federal do Rio De Janeiro COPPE/EE/IF, Rio de Janeiro; [(b)] Federal University of Juiz de Fora (UFJF), Juiz de Fora; [(c)] Federal University of Sao Joao del Rei (UFSJ), Sao Joao del Rei; [(d)] Instituto de Fisica, Universidade de Sao Paulo, Sao Paulo, Brazil
[25] Physics Department, Brookhaven National Laboratory, Upton NY, United States of America
[26] [(a)] National Institute of Physics and Nuclear Engineering, Bucharest; [(b)] University Politehnica Bucharest, Bucharest; [(c)] West University in Timisoara, Timisoara, Romania
[27] Departamento de Física, Universidad de Buenos Aires, Buenos Aires, Argentina
[28] Cavendish Laboratory, University of Cambridge, Cambridge, United Kingdom
[29] Department of Physics, Carleton University, Ottawa ON, Canada
[30] CERN, Geneva, Switzerland
[31] Enrico Fermi Institute, University of Chicago, Chicago IL, United States of America
[32] [(a)] Departamento de Física, Pontificia Universidad Católica de Chile, Santiago; [(b)] Departamento de Física, Universidad Técnica Federico Santa María, Valparaíso, Chile
[33] [(a)] Institute of High Energy Physics, Chinese Academy of Sciences, Beijing; [(b)] Department of Modern Physics, University of Science and Technology of China, Anhui; [(c)] Department of Physics, Nanjing University, Jiangsu; [(d)] School of Physics, Shandong University, Shandong, China
[34] Laboratoire de Physique Corpusculaire, Clermont Université and Université Blaise Pascal and CNRS/IN2P3, Clermont-Ferrand, France
[35] Nevis Laboratory, Columbia University, Irvington NY, United States of America
[36] Niels Bohr Institute, University of Copenhagen, Kobenhavn, Denmark
[37] [(a)] INFN Gruppo Collegato di Cosenza; [(b)] Dipartimento di Fisica, Università della Calabria, Arcavata di Rende, Italy
[38] AGH University of Science and Technology, Faculty of Physics and Applied Computer Science, Krakow, Poland
[39] The Henryk Niewodniczanski Institute of Nuclear Physics, Polish Academy of Sciences, Krakow, Poland
[40] Physics Department, Southern Methodist University, Dallas TX, United States of America
[41] Physics Department, University of Texas at Dallas, Richardson TX, United States of America
[42] DESY, Hamburg and Zeuthen, Germany
[43] Institut für Experimentelle Physik IV, Technische Universität Dortmund, Dortmund, Germany
[44] Institut für Kern- und Teilchenphysik, Technical University Dresden, Dresden, Germany
[45] Department of Physics, Duke University, Durham NC, United States of America
[46] SUPA - School of Physics and Astronomy, University of Edinburgh, Edinburgh, United Kingdom
[47] INFN Laboratori Nazionali di Frascati, Frascati, Italy
[48] Fakultät für Mathematik und Physik, Albert-Ludwigs-Universität, Freiburg, Germany
[49] Section de Physique, Université de Genève, Geneva, Switzerland
[50] [(a)] INFN Sezione di Genova; [(b)] Dipartimento di Fisica, Università di Genova, Genova, Italy
[51] [(a)] E. Andronikashvili Institute of Physics, Iv. Javakhishvili Tbilisi State University, Tbilisi; [(b)] High Energy Physics Institute, Tbilisi State University, Tbilisi, Georgia

JHEP01(2013)029

[52] II Physikalisches Institut, Justus-Liebig-Universität Giessen, Giessen, Germany
[53] SUPA - School of Physics and Astronomy, University of Glasgow, Glasgow, United Kingdom
[54] II Physikalisches Institut, Georg-August-Universität, Göttingen, Germany
[55] Laboratoire de Physique Subatomique et de Cosmologie, Université Joseph Fourier and CNRS/IN2P3 and Institut National Polytechnique de Grenoble, Grenoble, France
[56] Department of Physics, Hampton University, Hampton VA, United States of America
[57] Laboratory for Particle Physics and Cosmology, Harvard University, Cambridge MA, United States of America
[58] [(a)] Kirchhoff-Institut für Physik, Ruprecht-Karls-Universität Heidelberg, Heidelberg; [(b)] Physikalisches Institut, Ruprecht-Karls-Universität Heidelberg, Heidelberg; [(c)] ZITI Institut für technische Informatik, Ruprecht-Karls-Universität Heidelberg, Mannheim, Germany
[59] Faculty of Applied Information Science, Hiroshima Institute of Technology, Hiroshima, Japan
[60] Department of Physics, Indiana University, Bloomington IN, United States of America
[61] Institut für Astro- und Teilchenphysik, Leopold-Franzens-Universität, Innsbruck, Austria
[62] University of Iowa, Iowa City IA, United States of America
[63] Department of Physics and Astronomy, Iowa State University, Ames IA, United States of America
[64] Joint Institute for Nuclear Research, JINR Dubna, Dubna, Russia
[65] KEK, High Energy Accelerator Research Organization, Tsukuba, Japan
[66] Graduate School of Science, Kobe University, Kobe, Japan
[67] Faculty of Science, Kyoto University, Kyoto, Japan
[68] Kyoto University of Education, Kyoto, Japan
[69] Department of Physics, Kyushu University, Fukuoka, Japan
[70] Instituto de Física La Plata, Universidad Nacional de La Plata and CONICET, La Plata, Argentina
[71] Physics Department, Lancaster University, Lancaster, United Kingdom
[72] [(a)] INFN Sezione di Lecce; [(b)] Dipartimento di Matematica e Fisica, Università del Salento, Lecce, Italy
[73] Oliver Lodge Laboratory, University of Liverpool, Liverpool, United Kingdom
[74] Department of Physics, Jožef Stefan Institute and University of Ljubljana, Ljubljana, Slovenia
[75] School of Physics and Astronomy, Queen Mary University of London, London, United Kingdom
[76] Department of Physics, Royal Holloway University of London, Surrey, United Kingdom
[77] Department of Physics and Astronomy, University College London, London, United Kingdom
[78] Laboratoire de Physique Nucléaire et de Hautes Energies, UPMC and Université Paris-Diderot and CNRS/IN2P3, Paris, France
[79] Fysiska institutionen, Lunds universitet, Lund, Sweden
[80] Departamento de Fisica Teorica C-15, Universidad Autonoma de Madrid, Madrid, Spain
[81] Institut für Physik, Universität Mainz, Mainz, Germany
[82] School of Physics and Astronomy, University of Manchester, Manchester, United Kingdom
[83] CPPM, Aix-Marseille Université and CNRS/IN2P3, Marseille, France
[84] Department of Physics, University of Massachusetts, Amherst MA, United States of America
[85] Department of Physics, McGill University, Montreal QC, Canada
[86] School of Physics, University of Melbourne, Victoria, Australia
[87] Department of Physics, The University of Michigan, Ann Arbor MI, United States of America
[88] Department of Physics and Astronomy, Michigan State University, East Lansing MI, United States of America
[89] [(a)] INFN Sezione di Milano; [(b)] Dipartimento di Fisica, Università di Milano, Milano, Italy
[90] B.I. Stepanov Institute of Physics, National Academy of Sciences of Belarus, Minsk, Republic of Belarus
[91] National Scientific and Educational Centre for Particle and High Energy Physics, Minsk, Republic of Belarus
[92] Department of Physics, Massachusetts Institute of Technology, Cambridge MA, United States of America
[93] Group of Particle Physics, University of Montreal, Montreal QC, Canada

JHEP01(2013)029

[94] P.N. Lebedev Institute of Physics, Academy of Sciences, Moscow, Russia
[95] Institute for Theoretical and Experimental Physics (ITEP), Moscow, Russia
[96] Moscow Engineering and Physics Institute (MEPhI), Moscow, Russia
[97] Skobeltsyn Institute of Nuclear Physics, Lomonosov Moscow State University, Moscow, Russia
[98] Fakultät für Physik, Ludwig-Maximilians-Universität München, München, Germany
[99] Max-Planck-Institut für Physik (Werner-Heisenberg-Institut), München, Germany
[100] Nagasaki Institute of Applied Science, Nagasaki, Japan
[101] Graduate School of Science and Kobayashi-Maskawa Institute, Nagoya University, Nagoya, Japan
[102] [(a)] INFN Sezione di Napoli; [(b)] Dipartimento di Scienze Fisiche, Università di Napoli, Napoli, Italy
[103] Department of Physics and Astronomy, University of New Mexico, Albuquerque NM, United States of America
[104] Institute for Mathematics, Astrophysics and Particle Physics, Radboud University Nijmegen/Nikhef, Nijmegen, Netherlands
[105] Nikhef National Institute for Subatomic Physics and University of Amsterdam, Amsterdam, Netherlands
[106] Department of Physics, Northern Illinois University, DeKalb IL, United States of America
[107] Budker Institute of Nuclear Physics, SB RAS, Novosibirsk, Russia
[108] Department of Physics, New York University, New York NY, United States of America
[109] Ohio State University, Columbus OH, United States of America
[110] Faculty of Science, Okayama University, Okayama, Japan
[111] Homer L. Dodge Department of Physics and Astronomy, University of Oklahoma, Norman OK, United States of America
[112] Department of Physics, Oklahoma State University, Stillwater OK, United States of America
[113] Palacký University, RCPTM, Olomouc, Czech Republic
[114] Center for High Energy Physics, University of Oregon, Eugene OR, United States of America
[115] LAL, Université Paris-Sud and CNRS/IN2P3, Orsay, France
[116] Graduate School of Science, Osaka University, Osaka, Japan
[117] Department of Physics, University of Oslo, Oslo, Norway
[118] Department of Physics, Oxford University, Oxford, United Kingdom
[119] [(a)] INFN Sezione di Pavia; [(b)] Dipartimento di Fisica, Università di Pavia, Pavia, Italy
[120] Department of Physics, University of Pennsylvania, Philadelphia PA, United States of America
[121] Petersburg Nuclear Physics Institute, Gatchina, Russia
[122] [(a)] INFN Sezione di Pisa; [(b)] Dipartimento di Fisica E. Fermi, Università di Pisa, Pisa, Italy
[123] Department of Physics and Astronomy, University of Pittsburgh, Pittsburgh PA, United States of America
[124] [(a)] Laboratorio de Instrumentacao e Fisica Experimental de Particulas - LIP, Lisboa; [(b)] Departamento de Fisica Teorica y del Cosmos and CAFPE, Universidad de Granada, Granada, Spain
[125] Institute of Physics, Academy of Sciences of the Czech Republic, Praha, Czech Republic
[126] Faculty of Mathematics and Physics, Charles University in Prague, Praha, Czech Republic
[127] Czech Technical University in Prague, Praha, Czech Republic
[128] State Research Center Institute for High Energy Physics, Protvino, Russia
[129] Particle Physics Department, Rutherford Appleton Laboratory, Didcot, United Kingdom
[130] Physics Department, University of Regina, Regina SK, Canada
[131] Ritsumeikan University, Kusatsu, Shiga, Japan
[132] [(a)] INFN Sezione di Roma I; [(b)] Dipartimento di Fisica, Università La Sapienza, Roma, Italy
[133] [(a)] INFN Sezione di Roma Tor Vergata; [(b)] Dipartimento di Fisica, Università di Roma Tor Vergata, Roma, Italy
[134] [(a)] INFN Sezione di Roma Tre; [(b)] Dipartimento di Fisica, Università Roma Tre, Roma, Italy
[135] [(a)] Faculté des Sciences Ain Chock, Réseau Universitaire de Physique des Hautes Energies - Université Hassan II, Casablanca; [(b)] Centre National de l'Energie des Sciences Techniques Nucleaires, Rabat; [(c)] Faculté des Sciences Semlalia, Université Cadi Ayyad, LPHEA-Marrakech;

JHEP01(2013)029

[d] Faculté des Sciences, Université Mohamed Premier and LPTPM, Oujda; [e] Faculté des sciences, Université Mohammed V-Agdal, Rabat, Morocco
136 DSM/IRFU (Institut de Recherches sur les Lois Fondamentales de l'Univers), CEA Saclay (Commissariat a l'Energie Atomique), Gif-sur-Yvette, France
137 Santa Cruz Institute for Particle Physics, University of California Santa Cruz, Santa Cruz CA, United States of America
138 Department of Physics, University of Washington, Seattle WA, United States of America
139 Department of Physics and Astronomy, University of Sheffield, Sheffield, United Kingdom
140 Department of Physics, Shinshu University, Nagano, Japan
141 Fachbereich Physik, Universität Siegen, Siegen, Germany
142 Department of Physics, Simon Fraser University, Burnaby BC, Canada
143 SLAC National Accelerator Laboratory, Stanford CA, United States of America
144 [a] Faculty of Mathematics, Physics & Informatics, Comenius University, Bratislava; [b] Department of Subnuclear Physics, Institute of Experimental Physics of the Slovak Academy of Sciences, Kosice, Slovak Republic
145 [a] Department of Physics, University of Johannesburg, Johannesburg; [b] School of Physics, University of the Witwatersrand, Johannesburg, South Africa
146 [a] Department of Physics, Stockholm University; [b] The Oskar Klein Centre, Stockholm, Sweden
147 Physics Department, Royal Institute of Technology, Stockholm, Sweden
148 Departments of Physics & Astronomy and Chemistry, Stony Brook University, Stony Brook NY, United States of America
149 Department of Physics and Astronomy, University of Sussex, Brighton, United Kingdom
150 School of Physics, University of Sydney, Sydney, Australia
151 Institute of Physics, Academia Sinica, Taipei, Taiwan
152 Department of Physics, Technion: Israel Institute of Technology, Haifa, Israel
153 Raymond and Beverly Sackler School of Physics and Astronomy, Tel Aviv University, Tel Aviv, Israel
154 Department of Physics, Aristotle University of Thessaloniki, Thessaloniki, Greece
155 International Center for Elementary Particle Physics and Department of Physics, The University of Tokyo, Tokyo, Japan
156 Graduate School of Science and Technology, Tokyo Metropolitan University, Tokyo, Japan
157 Department of Physics, Tokyo Institute of Technology, Tokyo, Japan
158 Department of Physics, University of Toronto, Toronto ON, Canada
159 [a] TRIUMF, Vancouver BC; [b] Department of Physics and Astronomy, York University, Toronto ON, Canada
160 Faculty of Pure and Applied Sciences, University of Tsukuba, Tsukuba, Japan
161 Department of Physics and Astronomy, Tufts University, Medford MA, United States of America
162 Centro de Investigaciones, Universidad Antonio Narino, Bogota, Colombia
163 Department of Physics and Astronomy, University of California Irvine, Irvine CA, United States of America
164 [a] INFN Gruppo Collegato di Udine; [b] ICTP, Trieste; [c] Dipartimento di Chimica, Fisica e Ambiente, Università di Udine, Udine, Italy
165 Department of Physics, University of Illinois, Urbana IL, United States of America
166 Department of Physics and Astronomy, University of Uppsala, Uppsala, Sweden
167 Instituto de Física Corpuscular (IFIC) and Departamento de Física Atómica, Molecular y Nuclear and Departamento de Ingeniería Electrónica and Instituto de Microelectrónica de Barcelona (IMB-CNM), University of Valencia and CSIC, Valencia, Spain
168 Department of Physics, University of British Columbia, Vancouver BC, Canada
169 Department of Physics and Astronomy, University of Victoria, Victoria BC, Canada
170 Department of Physics, University of Warwick, Coventry, United Kingdom
171 Waseda University, Tokyo, Japan
172 Department of Particle Physics, The Weizmann Institute of Science, Rehovot, Israel

JHEP01(2013)029

[173] Department of Physics, University of Wisconsin, Madison WI, United States of America
[174] Fakultät für Physik und Astronomie, Julius-Maximilians-Universität, Würzburg, Germany
[175] Fachbereich C Physik, Bergische Universität Wuppertal, Wuppertal, Germany
[176] Department of Physics, Yale University, New Haven CT, United States of America
[177] Yerevan Physics Institute, Yerevan, Armenia
[178] Centre de Calcul de l'Institut National de Physique Nucléaire et de Physique des Particules (IN2P3), Villeurbanne, France

[a] Also at Laboratorio de Instrumentacao e Fisica Experimental de Particulas - LIP, Lisboa, Portugal
[b] Also at Faculdade de Ciencias and CFNUL, Universidade de Lisboa, Lisboa, Portugal
[c] Also at Particle Physics Department, Rutherford Appleton Laboratory, Didcot, United Kingdom
[d] Also at TRIUMF, Vancouver BC, Canada
[e] Also at Department of Physics, California State University, Fresno CA, United States of America
[f] Also at Novosibirsk State University, Novosibirsk, Russia
[g] Also at Department of Physics, University of Coimbra, Coimbra, Portugal
[h] Also at Department of Physics, UASLP, San Luis Potosi, Mexico
[i] Also at Università di Napoli Parthenope, Napoli, Italy
[j] Also at Institute of Particle Physics (IPP), Canada
[k] Also at Department of Physics, Middle East Technical University, Ankara, Turkey
[l] Also at Louisiana Tech University, Ruston LA, United States of America
[m] Also at Dep Fisica and CEFITEC of Faculdade de Ciencias e Tecnologia, Universidade Nova de Lisboa, Caparica, Portugal
[n] Also at Department of Physics and Astronomy, University College London, London, United Kingdom
[o] Also at Department of Physics, University of Cape Town, Cape Town, South Africa
[p] Also at Institute of Physics, Azerbaijan Academy of Sciences, Baku, Azerbaijan
[q] Also at Institut für Experimentalphysik, Universität Hamburg, Hamburg, Germany
[r] Also at Manhattan College, New York NY, United States of America
[s] Also at CPPM, Aix-Marseille Université and CNRS/IN2P3, Marseille, France
[t] Also at School of Physics and Engineering, Sun Yat-sen University, Guanzhou, China
[u] Also at Academia Sinica Grid Computing, Institute of Physics, Academia Sinica, Taipei, Taiwan
[v] Also at School of Physics, Shandong University, Shandong, China
[w] Also at Dipartimento di Fisica, Università La Sapienza, Roma, Italy
[x] Also at DSM/IRFU (Institut de Recherches sur les Lois Fondamentales de l'Univers), CEA Saclay (Commissariat a l'Energie Atomique), Gif-sur-Yvette, France
[y] Also at Section de Physique, Université de Genève, Geneva, Switzerland
[z] Also at Departamento de Fisica, Universidade de Minho, Braga, Portugal
[aa] Also at Department of Physics and Astronomy, University of South Carolina, Columbia SC, United States of America
[ab] Also at Institute for Particle and Nuclear Physics, Wigner Research Centre for Physics, Budapest, Hungary
[ac] Also at California Institute of Technology, Pasadena CA, United States of America
[ad] Also at Institute of Physics, Jagiellonian University, Krakow, Poland
[ae] Also at LAL, Université Paris-Sud and CNRS/IN2P3, Orsay, France
[af] Also at Nevis Laboratory, Columbia University, Irvington NY, United States of America
[ag] Also at Department of Physics and Astronomy, University of Sheffield, Sheffield, United Kingdom
[ah] Also at Department of Physics, Oxford University, Oxford, United Kingdom
[ai] Also at Department of Physics, The University of Michigan, Ann Arbor MI, United States of America
[aj] Also at Discipline of Physics, University of KwaZulu-Natal, Durban, South Africa
[ak] Also at Institute of Physics, Academia Sinica, Taipei, Taiwan
[*] Deceased

JHEP01(2013)029